Molecular mechanisms regulating Acc1 activity

Master Thesis

Florian Sarkleti, BSc

for attainment of the degree

Master of Science

MSc

Performed at the Institute of Molecular Biosciences

University of Graz

from May 2013 to April 2014

Supervision:

Univ.-Prof. Dr. Sepp D. Kohlwein

Dr. Harald F. Hofbauer

EIDESSTATTLICHE ERKLÄRUNG

Ich erkläre an Eides statt, dass ich die vorliegende Arbeit selbstständig verfasst, andere als die angegebenen Quellen/Hilfsmittel nicht benutzt, und die den benutzten Quellen wörtlich und inhaltlich entnommenen Stellen als solche kenntlich gemacht habe.

_____
Graz, 30.04.2014

place, date

_____

Florian Sarkleti, 0730341

STATUTORY DECLARATION

I declare that I have authored this thesis independently, that I have not used other than the declared sources / resources, and that I have explicitly marked all material which has been quoted either literally or by content from the used sources.

Graz, 30.04.2014

place, date

_____

Florian Sarkleti, 0730341

Danksagung

Mein aufrichtigster Dank ergeht an meine Eltern und meine Familie, die es mir ermöglicht haben dieses Studium zu absolvieren und mir immer Rückhalt und Unterstützung gewährt haben. Ohne sie wäre es mir nicht möglich gewesen diesen Weg einzuschlagen.

Des Weiteren möchte ich mich bei meiner Freundin Evelyn bedanken, die mir während meines Studiums und auch abseits davon immer zur Seite gestanden ist. Die wunderbare Zeit die ich mit dir verbracht habe hat mir immer neue Kraft gegeben.

Acknowledgements

I would like to express my gratitude to Prof. Sepp D. Kohlwein who gave me the opportunity to work in his lab and for supervising me during this thesis.

I also want to thank Dr. Harald F. Hofbauer for his continuous support and scientific guidance. His great enthusiasm and passion for science always encouraged me to give my best. Thank you Harry for all the time and effort you spent on guiding me through this work.

Further I thank Dr. Gerald N. Rechberger for his help during my project work, for his technical advices and for being a great colleague in the office.

And last but not least I would like to thank all the yeasty girls and boys for their support and the great time I had with you in this lab.

Molecular mechanisms regulating Acc1 activity

Florian Sarkleti, Harald F. Hofbauer and Sepp-Dieter Kohlwein

Institute of Molecular Biosciences, University of Graz

Acetyl-CoA carboxylase 1 (Acc1) catalyses the first and rate limiting step in *de novo* fatty acid synthesis which is highly conserved from unicellular microorganisms like yeast to higher eukaryotes. Acc1 uses acetyl-CoA to form malonyl-CoA, the building block of fatty acids. This essential reaction is regulated on various levels, underscoring the pivotal role of this enzyme in cellular lipid metabolism.

Due to its important role in fatty acid homeostasis Acc1 is a key player in several metabolic diseases such as obesity or cancer. A precise understanding of the underlying mechanisms regulating this enzyme can provide the basis for novel therapeutic approaches. However, the exact control mechanisms of Acc1 activity still have to be elucidated. Besides the known inactivation of Acc1 through phosphorylation by Snf1/AMPK and transcriptional regulation, recent studies provide evidence for a tertiary level of regulating Acc1 by increasing its activity through oligomerisation.

In this study we used yeast strains with differently GFP-tagged Acc1 fusion proteins and mutants bearing a non-phosphorylatable (hyperactive) Acc1 protein to investigate Acc1 protein levels, localisation and oligomerisation status depending on its intrinsic enzyme activity during growth in rich media.

Phenotypical characterisation revealed that the activity of Acc1 is differently affected depending on the GFP tag. The hyperactive Acc1 protein showed changes in localisation and oligomerisation status compared to wild type, while total protein levels remained unaltered. These findings confirm the proposed tertiary level of regulation in addition to transcriptional and post-translational control mechanisms. Furthermore, the localisation change of hyperactive Acc1 to the bud neck/septin ring in this strain indicates a possible role of Acc1 during cell division.

Immunostaining of untagged Acc1 protein and activity assays have to be further optimised to strengthen our findings.

Molekulare Mechanismen zur Regulation der Acc1 Aktivität

Florian Sarkleti, Harald F. Hofbauer und Sepp-Dieter Kohlwein

Institut für molekulare Biowissenschaften, Karl-Franzens-Universität Graz

Acetyl-CoA Carboxylase 1 (Acc1) katalysiert den geschwindigkeitsbestimmenden Schritt der *de novo* Fettsäurebiosynthese. Dieses Enzym ist hoch konserviert von einzelligen Mikroorganismen wie Hefe, bis zu höheren Eukaryoten. Acc1 nutzt Acetyl-CoA als Substrat um Malonyl-CoA zu synthetisieren, welches als Grundbaustein für Fettsäuren dient. Die Regulation dieser essentiellen Reaktion auf unterschiedlichsten Ebenen verdeutlicht die zentrale Rolle von Acc1 im Lipidstoffwechsel.

Aufgrund seiner Schlüsselrolle bei der Aufrechterhaltung des Fettsäuregleichgewichts nimmt Acc1 eine besondere Stellung in metabolischen Krankheiten wie Fettleibigkeit und Krebs ein, weshalb ein genaueres Verständnis der Regulationsmechanismen dieses Enzyms neue Ansätze für Therapiemöglichkeiten liefern kann. Neben der bekannten Inaktivierung von Acc1 aufgrund von Phosphorylierung durch die Kinase Snf1/AMPK und durch transkriptionelle Regulation, lieferten neueste Studien weitere Hinweise für eine dritte Regulationsebene, nämlich die Erhöhung der Acc1 Aktivität durch die Bildung von oligomeren Komplexen. Zur Aufklärung der Lokalisation, der Proteinmengen und des Oligomerisierungszustandes wurden Hefestämme mit unterschiedlich GFP-markierten Acc1 Fusionsproteinen und Mutanten mit nicht phosphorylierbarer (hyperaktiver) Acc1 verwendet. Die phänotypische Charakterisierung zeigte, dass unterschiedliche GFP-Markierung zu einer Beeinträchtigung der Acc1 Aktivität führt. Das hyperaktive Acc1 Enzym weist auf eine vom Wildtyp abweichende Lokalisierung und einen veränderten Oligomerisierungsgrad bei gleichbleibender Proteinmenge hin. Diese Resultate bestätigen das Vorhandensein einer weiteren Regulationsebene neben transkriptionellen und post-translationellen Kontrollmechanismen. Des Weiteren deutet eine Lokalisierung der hyperaktiven Acc1 zur Knospungsstelle/Septin Ring auf eine Beteiligung am Zellzyklus und der Zellteilung hin. Um diese Ergebnisse zu untermauern werden Immunostaining von nicht GFP-markierter Acc1 und *in vitro* Aktivitätstests weiter optimiert.

Content

Abbreviations

Abbreviation	Name
AB	antibody
Acc1	acetyl-CoA carboxylase 1
AMPK	AMP-activated protein kinase
BMI	body mass index
CL	cardiolipin
CoA	coenzyme A
DG	diacylglycerol
ER	endoplasmic reticulum
FA	fatty acid
FAME	fatty acid methyl ester
FAS	fatty acid synthase
FFA	free fatty acid
mGFP	monomeric green fluorscent protein
eGFP	enhanced green fluorscent protein
GPI	glycerophosphoinositol
LD	lipid droplet
NL	neutral lipid
PA	phosphatidic acid
PC	phosphatidylcholine
PE	phosphatidylethanolamine
PI	phosphatidylinositol
PL	phospholipid
PS	phosphatidylserine
SE	steryl ester
SL	sphingolipid
SorA	Soraphen A
TAG	triacylglycerol
UAS	upstream activating sequence
VLCFA	very long chain fatty acid
WHO	world health organistion

1 Introduction

Acetyl-CoA carboxylase 1 (Acc1) is the enzyme catalysing the first and rate determining step of the *de novo* FA synthesis (Hasslacher *et al.*, 1993) which makes it a key player in lipid metabolism. Acc1 is an essential enzyme which is highly conserved among all eukaryotic organisms and its activity is regulated at various levels, but the molecular mechanisms leading to this regulation are not fully understood. Furthermore, due to its pivotal role in lipid metabolism Acc1 can be related to severe diseases like obesity and cancer, which makes ACC1 a very attractive target to study novel methods and mechanisms to counteract such diseases. The idea of modulating Acc1 activity – besides the known effect of phosphorylation – through oligomerisation seems to be very promising to establish new treatment strategies.

1.1 Diseases related to lipid metabolism
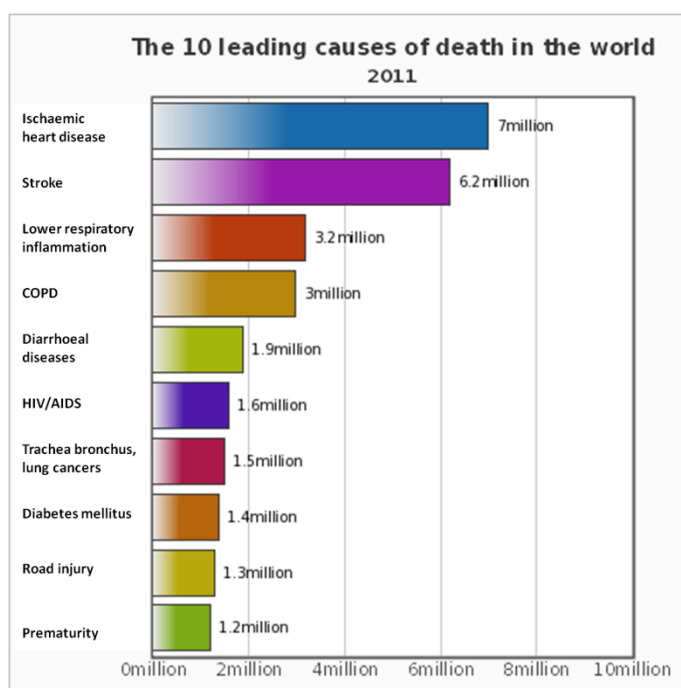
Figure 1: Causes of death. This top 10 list of worldwide death causes was published by the WHO in 2011 (WHO).

Causes of death depend on social and environmental conditions, but looking at the top 10 list of death causes, published by the World Health Organisation (WHO) in 2011, it turns out that diseases that can directly be linked to overweight and obesity are at the very top of this list. Especially in industrial countries ischaemic heart disease, stroke and diabetes cause massive problems that dramatically increased since 2000 and are still on the rise (WHO).

Rates of overweight and obesity are predicted to increase in almost all countries reaching 1.5 billion people who are overweight by 2015 (WHO). This fact is not very surprising as worldwide already 35% of adults are overweight and 12% are obese (WHO). In industrial countries it is even worse: in the United States of America 62% of the people are overweight and 26% are obese (WHO) and in Middle Europe 50% of the people are overweight and 20% are obese (WHO). The WHO actually claims obesity as one of the greatest public health problems of the 21st century (WHO), forcing the research on lipid metabolism to a necessity to face and counteract this serious threat. Moreover, another dangerous ailment that can slumber in every one of us and is responsible for 8.2 million deaths in the year 2012 has been related to lipid metabolism: cancer (WHO). Obesity does not cause cancer but, besides other factors, it dramatically increases the predisposition to develop cancer (WHO).

Obesity as well as cancer are disorders which are accompanied – or caused – by deregulated lipid metabolism that can simply be self-imposed by lack of exercise and malnutrition. On the other hand also genetic reasons or epigenetic defects due to environmental conditions lead to those severe diseases, putting them in the focus of extensive research in the last decades. However, many questions remain yet unanswered.

1.1.1 Obesity

The definition of obesity is based on a measure called body mass index (BMI). This BMI is defined by the equation BMI = $[\frac{kg}{m^2}]$. A BMI of ≥25 [kg/m^2] is considered as overweight, a BMI of ≥30 [kg/m^2] is referred to as obesity. To achieve a healthy lifestyle the WHO suggests a BMI in a range between 18.5 and 24.9 [kg/m^2]. Of course the BMI does not consider the composition of the body regarding the ratio of muscle to adipose tissue, but it is useful as a general indicator to easily and comparably classify a plethora of people (WHO).

There are several factors contributing to an increase in body weight. These factors are an imbalanced and excessive supply of nutrition, a so called high fat diet, mostly combined with a lack of physical activity. Additionally, dysfunctions in lipid metabolism can lead to an overproduction of FA and lipids which are stored in adipose tissue. Obesity causes severe problems that rise with an increase in the BMI and can finally even lead to death as mentioned before in the statistics of death causes.

The occurrence of hypertension, coronary heart disease and stroke, is mainly caused by a blockage of vessels due to lipid accumulation. Furthermore, the risk of gaining type 2 diabetes is promoted by overweight (WHO), and also Alzheimer's disease is thought to be more likely developed in adipose people (Lee, 2011; Hildreth *et al.*, 2012; Letra *et al.*, 2014).

1.1.2 Cancer

Not only these obvious health risks are related to a higher BMI as the WHO also states that the risk for cancer is increased by higher body weight (WHO). This connection becomes clearer by looking at the hallmarks that define cancer: unlimited cell growth, avoiding apoptosis and cell aging, induction of angiogenesis, invasion and metastasis, preventing immune destruction and changes in energy metabolism. These are factors that make previously normal, endogenous cells to cancer cells (Hanahan and Weinberg, 2000, 2011; Natter and Kohlwein, 2013). It is not surprising that the "excessive and lavish lifestyle" of cancer cells needs sufficient supply with metabolites. The demand for energy and resources for cell proliferation leads, amongst other things, to deregulated expression and activity of enzymes involved in lipid metabolism, especially in FA production. Acetyl-CoA carboxylase, an essential enzyme responsible for the rate limiting step in *de novo* FA synthesis, is proposed to play a key role in cancer progression (Beckers *et al.*, 2007).

1.1.3 Novel approaches to cure cancer

The challenge in cancer therapy is to destroy cancer cells as completely as necessary but thereby harming the healthy tissue as little as possible. Cancer cells are formerly normal, endogenous cells and, thus, hard to distinguish from healthy cells. However, the deregulations that turn them into immortal cancer cells on the other hand are their Achilles' heel, by making these cells unique and approachable for the development of cancer-specific drugs. Concerning lipid metabolism it turned out that a weak point of cancer cells seems to be their dependence on *de novo* synthesised FA, whereas normal cells largely rely on external FA supply (Chajès *et al.*, 2006; Beckers *et al.*, 2007). Several studies already showed the potential of drugs affecting lipid metabolism especially in cancer cells (Pizer *et al.*, 1996b; Brusselmans *et al.*, 2005; Beckers *et al.*, 2007; Wang *et al.*, 2009).

The upregulation of enzymes involved in lipid metabolism includes acetyl-CoA carboxylase 1 (Acc1/ACC1), the rate limiting enzyme of *de novo* FA synthesis. Acc1 produces malonyl-CoA, which is further used by the fatty acid synthase complex (FAS/FASN) to generate saturated FA. Both enzymes are overexpressed in cancer cells at the very beginning of development and their levels even increase during cancer progression (Beckers *et al.*, 2007).

The dependence of *de novo* FA synthesis was already used as an approach to decrease cancer cell viability. For example, the inhibition of FASN by different compounds like cerulenin or orlistat leads to an increase of malonyl-CoA and a decrease of fatty acids. The excess of this intermediate was reported to be toxic for the cell, and treatment with these drugs specifically results in apoptosis of tumor cells (Pizer *et al.*, 1996a, 1996b; Kuhajda, 2000; Kridel *et al.*, 2004; Bandyopadhyay *et al.*, 2006; Johansson *et al.*, 2008).

Another novel approach is dealing with the inhibition of FA production even one step before the FA synthase complex. Beckers and coworkers showed that decreasing Acc1 activity with the specific allosteric inhibitor Soraphen A leads to an insufficient supply with malonyl-CoA and, thus, a lack of FA in cancer cells. This treatment decelerates proliferation and induces cell death selectively in cancer cells (Chajès *et al.*, 2006; Beckers *et al.*, 2007).
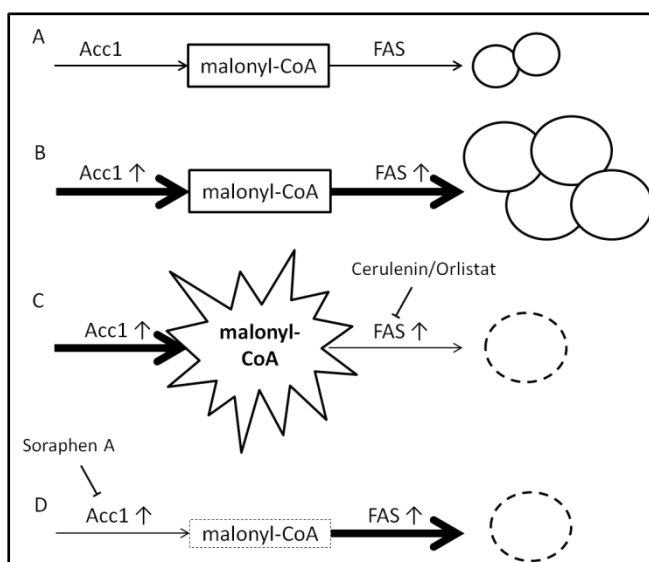
Figure 2: Deregulated *de novo* FA synthesis. (A) shows balanced Acc1 and FAS levels and normal cell growth. (B) upregulation of Acc1 and FAS is needed for the elevated cell growth in cancer cells. Deregulation of malonyl-CoA levels either by blocking FAS (C) or Acc1 (D) leads to reduced cell viability.

In Figure 2 the proposed processes are graphically shown. Under physiological conditions (A) the flux of malonyl-CoA is regulated in a balanced way, which is also the case in tumor cells (B).

Although both enzymes show higher activity for a higher production of FA, the net formation and consumption of malonyl-CoA is still balanced. When an imbalance in this flux is induced, either by blocking of FAS (C) or Acc1 (D), the surplus or the lack of malonyl-CoA is strongly believed to lead to a toxic condition for the cell.

In conclusion, the production of malonyl-CoA has to be very tightly regulated to ensure an appropriate level of FA. We suggest that the cellular regulation steps mainly occur on the level of malonyl-CoA production and not on its consumption. There is no obvious sense for a cell to increase FAS activity to gain more FA when Acc1 does not provide enough substrate or to decrease FAS activity when Acc1 activity is still unaltered, leading to accumulation of malonyl-CoA. This hypothesis is underlined by the facts that Acc1 is known to be the rate-limiting step in *de novo* FA synthesis and that deletion of FAS can be rescued by exogenous supply of FA (Tehlivets *et al.*, 2007), whereas inhibition of Acc1 cannot (Hasslacher *et al.*, 1993; Vahlensieck *et al.*, 1994; Shirra *et al.*, 2001). Based on that it is necessary to clarify which other mechanisms regulate Acc1 activity to understand and counteract lipid related diseases, especially cancer.

1.2 Cellular lipid composition is crucial for cell viability

Studies revealed that the composition of lipids decisively affect cell viability (Hofbauer, 2012) and deregulations in the formation processes can directly be related to severe diseases as discussed above (see chapter 1.1). Furthermore, Hofbauer et al. showed that the homeostasis of a certain FA composition is required not only to form stable membranes but additionally affects the transcription of essential genes for phospholipid synthesis. Acc1 is the key enzyme in the *de novo* FA synthesis determining the amount but also the chain length of FA and thereby lipid composition. [Hofbauer et al., 2014, in prep.]. To understand the consequences of a deregulated lipid metabolism it is essential to know about the function of lipids and their FA precursors.

Lipids are essential metabolites in all living species. In eukaryotic organisms they cover a large spectrum of functions which can be subdivided into anabolic and catabolic processes. In anabolic processes lipids are used as building blocks for the synthesis of other molecules in an energy dependent manner.

This part of lipid metabolism includes the provision of fatty acids (FAs) for the synthesis of components needed for membrane formation, which is essential for cell viability and proliferation. Furthermore FAs are used for hormone production and play an important role in protein modification and signalling processes. In times of excess nutrients, FAs can be stocked in special storage lipids which exhibit a high energy content. These storage compounds secure the survival of cells during nutritional shortages. The catabolic pathway describes the breakdown of complex lipids and FAs to yield energy and FAs which in turn provide the basis for further anabolic processes.

Lipids serve as a very potent energy source and provide a long term storage form of energy besides glycogen and starch. They are used for membrane formation and homeostasis as well as for signalling processes. Lipids can be divided into different species according to their structure as described in the next chapters.

1.2.1 Fatty acids (FA)

The most simple lipid species are fatty acids, which consist of a carboxyl head group and an acyl chain of variable length. An additional structural feature is the number and position of double bonds in the acyl chain which consists of an even number of C atoms in most eukaryotes, whereas prokaryotes also bear odd chained FA. Formation of odd chain FA can be achieved by starting FA synthesis with propionyl-CoA instead of acetyl-CoA (see also section FA synthesis). Yeast has a FA spectrum mainly consisting of C16 and C18 FA, with 70-80% of all FA being monounsaturated at the Δ9 position (Martin *et al.*, 2007; Tehlivets *et al.*, 2007). Besides these major FA species, minor species such as C12:0, C14:0, C14:1, C20:0, C22:0, C24:0 and C26:0 are found in yeast and have important functions in protein modifications, as components of sphingolipids and GPI anchors.

A balanced FA contribution, achieved mainly by *de novo* FA synthesis, seems to be essential for cell viability, which highlights the importance of the tightly regulated Acc1 activity.
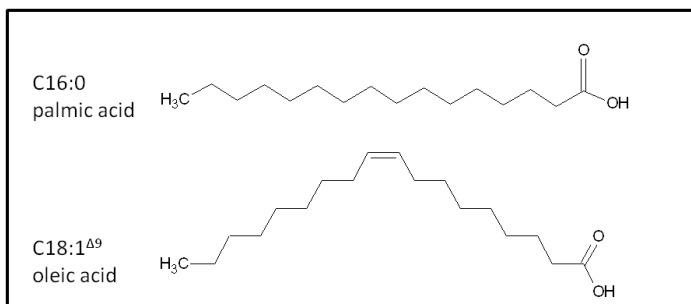
Figure 3: Examples of fatty acids. The figure shows a saturated C16:0 FA and an unsaturated C18 FA with a cis-double bond at the Δ9 position, introducing a kink in the carbon chain. The first number indicates the number of C atoms of the carbon chain, the second number stands for the number of double bonds. Δ9 defines the position of the double bond, counted from the carboxyl group.

1.2.2 Phospholipids (PL)

Phospholipids are amphiphilic molecules with two FA esterified to the *sn1* and *sn2* positions of a glycerol backbone. These FA are termed hydrophobic tails of the phospholipid. The *sn3* position of the glycerol backbone is esterified with a phosphate group yielding the simplest PL molecule termed phosphatidic acid (PA). The phosphate group is further modified by various substituents which define the phospholipid class (Figure 4). The most abundant phospholipids are phosphatidylcholine (PC), phosphatidylethanolamine (PE), phosphatidylinositol (PI) phosphatidylserine (PS) and cardiolipin (CL). Sphingomyelins represent another type of phospholipid bearing a sphingosine backbone instead of glycerol. Due to their amphiphilic character phospholipids are mainly used for the formation of all kinds of membranes in the cellular environment. The degree of desaturation of the FA tails is used to balance membrane fluidity, a key feature to sustain cell viability under variable environmental conditions (de Kroon *et al.*, 2013).

Figure 4: Phospholipid classes: The marked head goups define the major classes of phospholipids in yeast, the FA tails determine the PL species. The kink introduced by cis-double bonds leads to disorderd structures in the phospholipid membrane and hence to higher membrane fluidity. The residues R in CL represent the carbon chains of FA.

1.2.3 Neutral lipids (NL)

Another important lipid family consists of neutral lipids (NL) such as triacylglycerols (TAG), diacylglycerols (DAG) and steryl esters (SE). TAG contains a glycerol backbone where all three hydroxyl groups are esterified to FAs, whereas in DAG only two positions are linked to FA. In SE the hydroxy group of a sterol is esterified with a single FA (Figure 5). TAG and SE can be tightly packed into so called lipid droplets (LD) and are important storage compounds. In times of energy scarcity the NL are hydrolysed and the free FAs are used as energy source. The free FA derived from NL hydrolysis can also be used as building blocks for PL synthesis and cell proliferation.

Figure 5: Neutral lipids. TAG, DAG and SE are the main NL classes. The species are determined by the hydrophobic FA tails.

More than 21 classes of lipids consisting of over 250 species in total have already been identified in *Saccharomyces cerevisiae* (Ejsing *et al.*, 2009). In mammals the lipid composition is even more complex with way more than 300 lipid species within 14 different lipid classes (Sampaio *et al.*, 2011). The relatively simple lipid composition in yeast combined with the highly conserved *de novo* FA synthesis pathway offers an excellent model system to investigate the lipid metabolism as discussed in the next chapter.

1.3 Yeast as a model organism

Metabolic reactions and regulatory mechanisms are largely conserved across the whole eukaryotic kingdom, reaching from single cell organisms like yeast over mice to multicellular organisms like humans. *De novo* FA synthesis including the reaction catalysed by Acc1 is one such highly conserved pathway which allows the implementation of studies in selected model scenarios in yeast without ethical considerations (Natter and Kohlwein, 2013). The obtained findings can provide insights into human disorders and diseases and serve as basis for new therapeutical approaches (Sherman, 2002).

However, in contrast to multicellular organisms or mammalian cell lines, the yeast *Saccharomyces cerevisiae* has several advantages that highlight it as an attractive model organism; (i) the whole yeast genome is sequenced and accessible which facilitates genetic manipulations, (ii) large mutant collections are already available and physiology and metabolism are well understood, (iii) there are almost no quantitative limitations in cultivating the cells as they have a short generation time and are easy and safe to handle (Sherman, 2002). Yeast, which usually grows in colonies, also shows multicellular behaviour like apoptosis and physiological differentiation of cells within one colony (Carmona-Gutierrez *et al.*, 2010; Cáp *et al.*, 2012; Natter and Kohlwein, 2013). Beyond that fermenting yeast shares similarities to the metabolic reprogramming in cancer cells and, therefore, induced deregulations in the highly conserved lipid metabolism can serve as an ideal basis for studying mechanisms of cancer physiology in yeast. Nevertheless, besides the advantages of yeast one has to always keep in mind that there are differences to higher, multicellular eukaryotes, and mechanisms revealed in yeast have to be carefully validated before they are transferred to elucidate mechanisms in human cells (Botstein and Fink, 2011; Hofbauer, 2012). Figure 6 shows a general overview of the lipid metabolism pathway in yeast which is highly conserved in the eukaryotic kingdom.
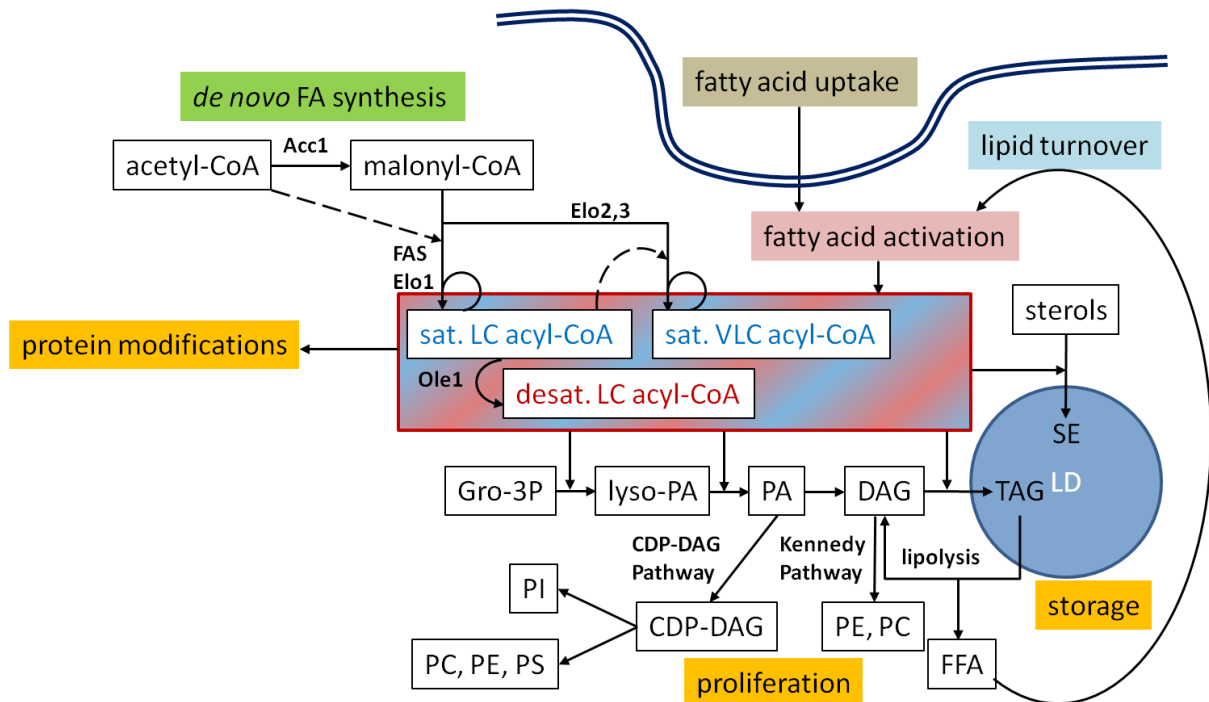
Figure 6: Lipid metabolism in yeast. This figure provides an overview of the lipid metabolic pathway in yeast.

1.4 FA synthesis in yeast

As mentioned above, FA and the derived lipids are of essential importance for the cell. There are three ways known how yeast obtains FA: lipid turnover, exogenous uptake and *de novo* FA synthesis. Lipid turnover and lipolysis are continuous processes within the yeast cell, providing FA from degraded neutral- and phospholipids to maintain lipid homeostasis (Boumann *et al.*, 2006; Gaspar *et al.*, 2011). This is rather a conversion process of already existing lipids and not practicable for increasing FA and lipid amount. Yeast has two other ways to provide the cells with a sufficient quantity of FA: One is the uptake of exogenous FA, but although yeast has the ability to take up FA from the environment quite efficiently, it is usually independent of FA as a natural feeding source. Additionally, the free fatty acids (FFA) derived from lipid turnover or exogenous uptake are toxic for the cell and have to be activated with coenzyme-A before they can be further utilised (Zou *et al.*, 2003; Black and DiRusso, 2007). Hence, the third way, endogenous *de novo* FA synthesis, is the main supplier of activated FA in yeast (Tehlivets *et al.*, 2007).

The two enzymes carrying out the reactions in the *de novo* FA synthesis pathway are acetyl-CoA carboxylase 1 (Acc1) and the FAS complex. Acc1 catalyses the first and rate limiting step from acetyl-CoA to malonyl-CoA which is then further used by the FAS complex (together with Elo1) for the elongation of either acetyl-CoA or acyl-CoA in a circular process to yield long chain fatty acyl-CoA. Every step of this reaction needs one molecule of malonyl-CoA to elongate the growing carbon chain by two CH_2 units. Formation of malonyl-CoA by Acc1 is an activation process of acetyl-CoA with CO_2, since elongation by FAS only needs two CH_2 units and releases CO_2. If very long chain FA (VLCFA) are required, especially for the formation of the cermide backbone in sphingolipids, the long chain acyl-CoAs are elongated by Elo2 and Elo3 in a similar way like FAS, using malonyl-CoA to extend the existing carbon chain by two CH_2 units, and up to a length of 26 carbon atoms (Tehlivets *et al.*, 2007; Henry *et al.*, 2012).

All *de novo* synthesised FAs are fully saturated. The activated FA from exogenous uptake or lipid turnover can be saturated, but to maintain membrane stability and fluidity a certain extent of desaturation is necessary. Yeast has only one single enzyme to catalyse the desaturation of all FA, namely Ole1, a desaturase which introduces a cis-double between the C9 and C10 position of FAs, no matter if they are *de novo* synthesised or taken up (Tatzer *et al.*, 2002; Martin *et al.*, 2007; De Smet *et al.*, 2012).

The produced acyl-CoAs are then esterified to glycerol-3-phosphate to form lysoPA and PA which can be converted to DAG by hydrolysis of the phosphate head group. PL can be derived independently either from PA or DAG via two different pathways which are both used in yeast (Patton-Vogt *et al.*, 1997; Henry *et al.*, 2012). PA is the substrate for the so called CDP-DAG pathway whereas DAG is used in the Kennedy pathway. Additionally, DAG can be esterified with one more acyl-CoA chain to yield TAG. Attaching acyl-CoA to sterols yields steryl esters which are stored together with TAG in compartments known as lipid droplets for times of energy or FA depletion.

The importance of *de novo* FA synthesis with regard to cancer and its upregulation in tumor cells has already been discussed above. However, inhibition of FA synthesis by deletion of *FAS1* and *FAS2* (encoding the subunits of the FAS complex)*,* which is lethal on standard media, can be rescued by exogenous supply of long chain fatty acids (Winzeler *et al.*, 1999; Tehlivets *et al.*, 2007).

In contrast to the FAS complex, impairing Acc1 activity by deletion or inhibition with SorA has been shown to be lethal even in the presence of long chain FA since the produced malonyl-CoA is also the substrate to generate the essential VLCFA (Hasslacher *et al.*, 1993; Vahlensieck *et al.*, 1994; Shirra *et al.*, 2001). The next chapter is focusing on how this enzyme is regulated, also highlighting its pivotal role in lipid metabolism.

1.5 Spotlight on acetyl-CoA carboxylase (Acc1)

ACCs are found in all living organisms from bacteria or single cell fungi over plants and animals up to humans. They have evolved from multi-subunit enzymes in bacteria like *E. coli* and plants, where three single peptide subunits interact to form a functional holoenzyme, to multi-domain proteins in eukaryotes, where one protein harbours all domains needed for enzyme activity. Eukaryotic Acc1 is such a multi-domain protein consisting of a biotin carboxylase domain (BC), a biotin carboxyl carrier protein domain (BCCP) and a carboxyl transferase domain (CT). These domains are highly conserved among all eukaryotic organisms. Human BC and CT domain of ACC1 show sequence identity to the yeast BC and CT domains of 63% and 49%, respectively. However, there are small differences between these two species regarding Acc1 structure. Human ACC1 consists of 2346 amino acid residues, with a weight of 265 kD. Yeast Acc1 is composed of 2233 amino acids with a molecular weight of 250 kD, and it lacks a phosphorylation site at position 79 which was repeatedly described to be involved in the AMPK-dependent regulation of human ACC1 activity (Davies *et al.*, 1990; Munday, 2002; Tong, 2005; Tong and Harwood, 2006; Locke *et al.*, 2008). Nevertheless, other phosphorylation sites at position 1200 and 1215 are proposed to be important for human ACC1, and in yeast a single phosphorylation site was identified at serine 1157 (Ha *et al.*, 1994; Hofbauer, 2012). Unfortunately the three dimensional structure of any acetyl-CoA carboxylase is not resolved yet. Due to its size it is unsuitable for NMR analysis and so far no crystal structure of the whole protein is available. However, the BC and CT domains have independently been crystallised and the structures were used for first inhibitor studies (Zhang *et al.*, 2003; Shen *et al.*, 2004; Tong and Harwood, 2006). Another structural feature of yeast Acc1 is a prominent coiled-coil domain in the C-terminal part of the enzyme between AA 2034–2064 (Tehlivets *et al.*, 2007). Such coiled-coil domains are indicators for protein-protein interactions.

In solution the smallest active form of Acc1 that is found is a dimer (Kim *et al.*, 2010) and inhibitor studies propose that dimerisation occurs at the BC domain (Shen *et al.*, 2004). Furthermore, biotinylation of Acc1 at lysine 735 by the essential enzyme biotin-apoprotein ligase (Bpl1/Acc2) is required to form an active enzyme (Mishina *et al.*, 1980; Toh *et al.*, 1993; Schneiter *et al.*, 1996).
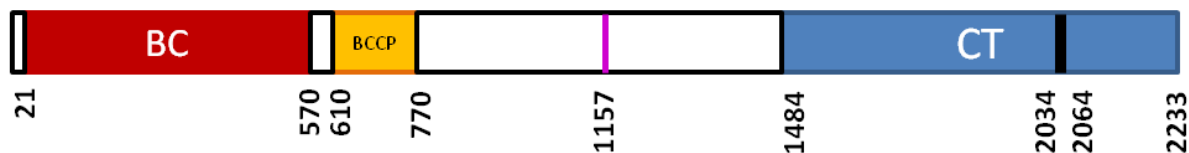
Figure 7: Acc1 protein. Acc1 consists of three main domains: The biotin carboxylase (BC) domain at the N-terminus, the biotin carboxyl carrier protein (BCCP) domain and the carboxyl transferase (CT) domain at the C-terminus. The CT domain bears a prominent coild coil domain between AA 2034 and AA 2064. The only known phosphorylation site is located at position 1157, in a part without any known function in the middle of the enzyme.

In mammals an isoform of ACC1, named ACC2, is found in the outer mitochondrial membrane of heart and muscle cells. The malonyl-CoA produced by ACC2 inhibits carnitine palmitoyltransferase which is responsible for the transport of long chain acyl-CoAs into the mitochondria for β-oxidation. This feedback mechanism prevents FA degradation in times when *de novo* FA synthesis is switched on and acyl-CoAs are synthesised. The yeast ortholog of ACC2, Hfa1, is also localised to mitochondria. Interestingly, both the yeast and mammalian protein lack the phosphorylation site at position 1157 and 1200, respectively.

1.5.1 Functions of Acc1 domains

Acc1 is a biotin dependent multi-domain protein and catalyses the formation of malonyl-CoA from acetyl-CoA. This process can be divided into single reactions carried out by the different domains of the protein.

The reaction cascade starts with the ATP-dependent carboxylation of the biotin moiety at the BC domain of Acc1. Bicarbonate serves as a donor of the carboxyl group and is activated by the γ-phosphate of ATP in the presence of bivalent cations such as Mg^{2+}. The activated intermediate is used to form carboxybiotin, which translocates to the CT domain. This nominal transport of CO_2 from the BC to the CT domain is mediated by the long and flexible biotin arm, which is covalently attached to the BCCP domain. At the CT domain, the activated CO_2 in the form of carboxybiotin reacts with the methyl group of acetyl-CoA to form malonyl-CoA which is then released to the cytosol (Tong, 2005; Chou *et al.*, 2009).
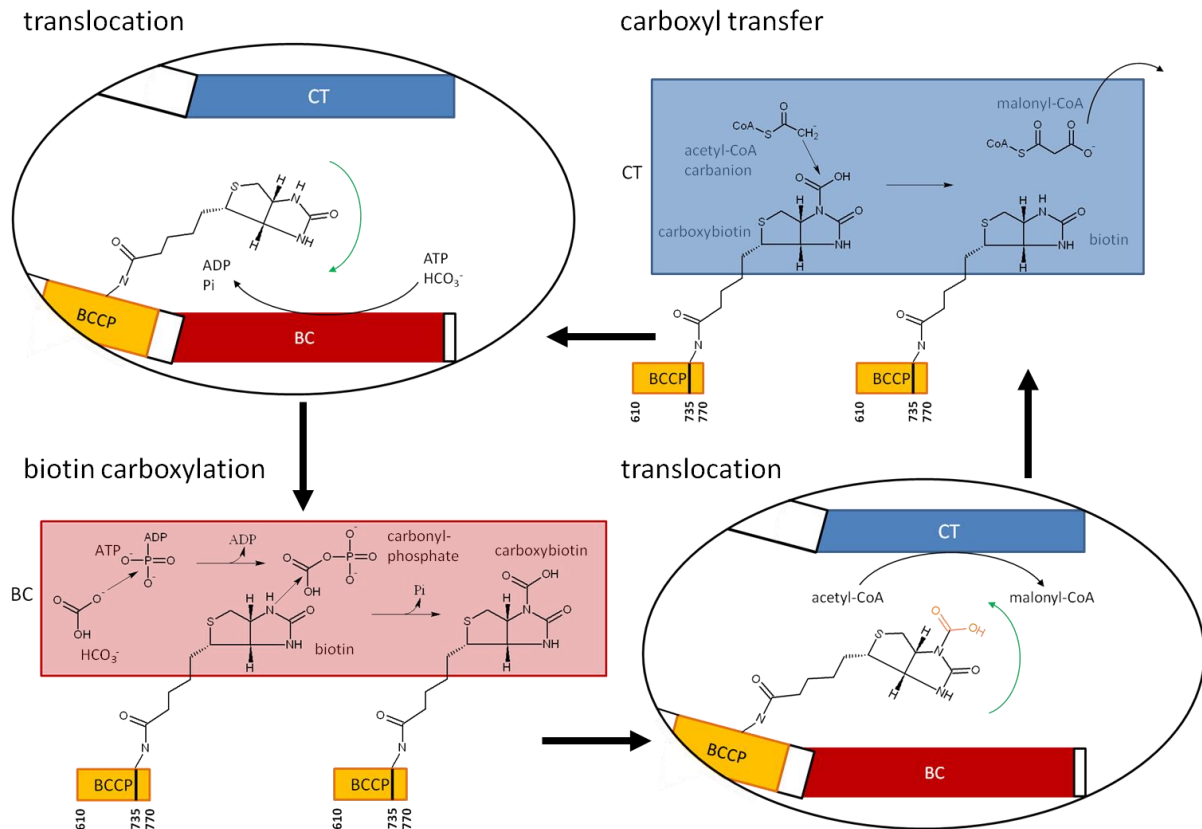
Figure 8: Acc1 reaction cycle. Biotin translocates to the BCCP and gets carboxylated at the BC domain. The carboxylated biotin then translocates to the CT domain and provides CO_2 for the formation of malonyl-CoA from acetyl-CoA. Malonyl-CoA is released to the cytosol and the reaction cycle starts again. Adapted from Tong, 2005 (Tong, 2005).

1.5.2 Functions of Acc1 besides *de novo* FA synthesis

Besides the main function as supplier of malonyl-CoA in *de novo* FA synthesis, Acc1 was found to be indirectly involved in other important processes like histone acetylation and cell cycle progression. For the production of malonyl-CoA, Acc1 consumes acetyl-CoA which is also used by histone acetyltransferases. Both reactions obtain acetyl-CoA from the nuleocytosolic pool and, thus, compete for the same substrate. This competition for a limited amount of substrate allows Acc1 to indirectly regulate histone acetylation to a certain extent and links lipid metabolism to transcriptional regulation (Galdieri and Vancura, 2012; Zhang *et al.*, 2013).

Moreover, a connection of Acc1 to cell cycle progression was observed in a temperature sensitive Acc1 mutant. Decreasing Acc1 activity in this strain resulted in a cell cycle arrest at the G2/M phase, which could not be supressed by external supply of FA to the media (Al-Feel *et al.*, 2003). In support of this, Vazquez-Martin and co-workers show that mammalian ACC1, when phosphorylated at serine 79, localises to the spindle pole in lung carcinoma cells (Vazquez-Martin *et al.*, 2013).

This indicates that Acc1 plays an essential role in cell cycle progression, possibly by providing malonyl-CoA for VLCFA and subsequently sphingolipid synthesis.

1.5.3 Regulation of Acc1 activity

1.5.3.1 Long term regulation

Due to its crucial metabolic function, Acc1 is tightly regulated at various levels. The long term regulation of the mammalian ACC1 protein, with a half-life of 1-3 days, is achieved by regulating the protein amount at the level of transcription (Munday, 2002). In yeast, Acc1 is highly expressed in the logarithmic growth phase (Lampl, 1998) and controlled via an autoregulatory feedback loop sensing the amount of produced long chain fatty acyl-CoAs. Literature provides evidence that exogenous C16:1 supply decreases mRNA levels significantly (Shirra *et al.*, 2001). Furthermore, Acc1 is under the control of a sequence in the promoter region termed as UAS_{INO} (inositol sensitive upstream activating element; Chirala et al., 1994; Hasslacher et al., 1993; Tehlivets et al., 2007). The regulation is achieved by the transcription activators Ino2/Ino4 and the repressor Opi1 in response to PA levels as signalling factor (Carman and Han, 2009; Henry *et al.*, 2012). Opi1 binds to PA at the nuclear ER and attaches it to the ER membrane. This allows the transcription of genes under UAS_{INO} control when inositol levels are low and little PI is produced. In the presence of inositol PI synthesis is switched on, PA is consumed and does no longer bind Opi1, which in turn is released from the ER, translocates into the nucleus and inhibits the transcription of genes under UAS_{INO} control (Figure 9).
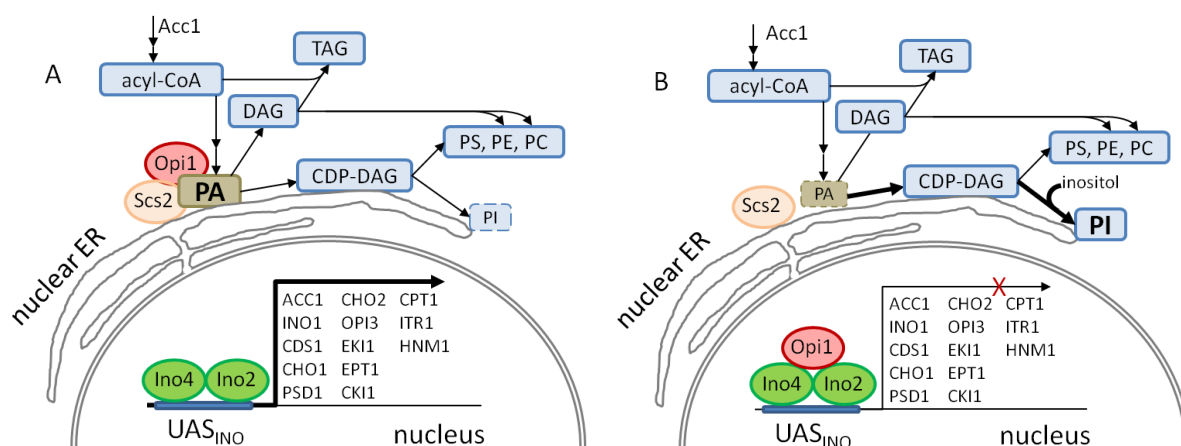
Figure 9: Transcriptional regulation by inositol. Gene transcription is enabled when inositol is depleted and PA can bind the repressor Opi1 to the nuclear ER (A). When inositol is added, the production of PI increases and PA is consumed, which leads to translocation of Opi1 from the ER into the nucleus and transcription of phospholipid biosynthetic genes is inhibited (B).

The fact that transcription of *ACC1* and *INO1* are regulated by the same mechanism, links inositol auxotrophy to high Acc1 activity as also described in literature (Shirra *et al.*, 2001). The proposed model that high Acc1 activity leads to an increased TAG production and hence a decrease in PA levels and an Ino⁻ phenotype was proven to be wrong as PA levels rather increased in a mutant bearing a hyperactive Acc1 allele. Hofbauer and co-workers now provide evidence that not only total PA amount but also PA species composition play a key role in the expression of genes under UAS_{INO} via the Ino2/Ino4/Opi1 regulatory circuit. [Hofbauer et al., 2014, in prep.]

1.5.4 Short term regulation

Short term regulation is carried out at the protein level by post-translational modifications. Phosphorylation is known to inhibit Acc1 activity and several phosphorylation sites have been identified. In mammalian ACC1 serine residues at position 79, 1200 and 1215 are known to be phosphorylated either by AMP activated protein kinase (AMPK) or 5´cAMP dependent protein kinase (Ha *et al.*, 1994). As mentioned above yeast lacks the phosphorylation site at position 79 and phosphoproteome studies revealed a single phosphorylation site at serine 1157 which is embedded in a consensus motif for Snf1, the yeast ortholog of mammalian AMPK (Woods *et al.*, 1994; Shirra *et al.*, 2001; Ficarro *et al.*, 2002; Brinkworth *et al.*, 2006). Recently it was shown that in logarithmically growing wild type yeast cells, 70% of Acc1 is phosphorylated at serine 1157 and that deletion of Snf1 kinase decreases the phosphorylation level by half [Hofbauer et al., 2014, in prep.].

1.5.5 Regulation through oligomerisation

The smallest active form of Acc1 is reported to be a homodimeric complex (Kim *et al.*, 2010). It has been shown that an increasing number of Acc1 molecules in this complex leads to highly increased activity and thus provides an additional short term regulatory mechanism (Numa *et al.*, 1965; Thampy and Wakil, 1985; Borthwick *et al.*, 1987; Munday, 2002; Locke *et al.*, 2008; Kim *et al.*, 2010). Citrate was reported to support this polymerisation process *in vitro* in mammalian cells, but the *in vivo* role of citrate was questioned because the required concentrations to show effects by far exceeded the physiological levels (Thampy and Wakil, 1985).

Recently, Kim and co-workers published a novel polymerisation mechanism to increase Acc1 activity in liver cells at physiological citrate levels. They discovered that Acc1 polymerisation is initiated by MIG12, a protein that is subsequently incorporated into the complex (Kim *et al.*, 2010). A putative antagonist of MIG12 is SPOT14, a lipogenesis-related nuclear protein, which forms heterodimers with its paralog MIG12. This heterodimeric complex has been shown to reduce polymerisation, and hence activity, of both ACC1 and ACC2, indicating a regulatory role in lipid metabolism (Colbert *et al.*, 2010; Park *et al.*, 2013). Additionally, a possible role in breast cancer growth and survival was suggested for SPOT14 (Martel *et al.*, 2005).

This regulatory mechanism provides a very promising approach for manipulating ACC activity with regard to treatment of obesity and cancer. However, no orthologs of these proteins in yeast have been described so far.

1.5.6 Chemical inhibition

Besides the cellular regulation mechanisms, molecules that inhibit the function of acetyl-CoA carboxylase have been identified and were especially discovered as fungicides and herbicides for commercial usage. One well explored compound specifically inhibiting eukaryotic ACC is Soraphen A, which belongs to the group of naturally occurring macrocyclic polyketides and is isolated from the bacterium *Sorangium cellulosum* (Shen *et al.*, 2004; Jump *et al.*, 2011). It binds to the BC domain of ACC and inhibits the dimerisation of these subunits, thus preventing the formation of highly oligomeric structures and impairing ACC activity (Vahlensieck *et al.*, 1994; Shen *et al.*, 2004; Weatherly *et al.*, 2004; Jump *et al.*, 2011).

1.6 Hypothesis and aims

The aim of this study was to answer the question whether Acc1 activity can be connected to the oligomerisation state of Acc1 and if the formation of oligomeric Acc1 complexes represents a possible regulatory mechanism. Furthermore, we attempted to show the localisation of Acc1 depending on its activity and phosphorylation state during the different phases of growth. It is proposed in the literature that the smallest active form of Acc1 is a homodimer and the activity is increased by oligomerisation. However, as far as we know no proper model why and how oligomerisation increases Acc1 activity is proposed.

Based on that we aimed for showing oligomerisation of Acc1 in vivo, using differently GFP tagged Acc1 mutants in wild type and hyperactive Acc1 background. To validate the best tagging strategy with regard to native behaviour we performed phenotypic characterisation experiments on media containing the Acc1 inhibitor Soraphen A (SorA). The connection of inositol auxotrophy and hyperactivity of Acc1 as well as overproduction of inositol in strains with low Acc1 activity in combination with SorA treatment to modulate Acc1 activity should extend the characterisation profile. To confirm the localisation obtained by GFP tagging, cells bearing native Acc1 were subjected to immune fluorescence labelling and confocal laser scanning microscopy. Furthermore, we used lipid analysis to indirectly measure Acc1 activity in the different mutant strains. To show oligomeric complexes on the protein level and to finally connect oligomerisation and the previously determined Acc1 activity we used native gradient gel PAGE and Western blot analysis.

2 Results

2.1 Work flow

Acc1 is regulated at multiple levels but to answer the question how oligomerisation influences Acc1 activity and if any localisation changes arise due to changes in Acc1 activity we came up with the work flow shown below. We used differently GFP-tagged Acc1 and confocal laser scanning microscopy to unveil Acc1 localisation, lipid analysis and plate tests to reveal Acc1 activity, native gradient polyacrylamide gel electrophoresis (PAGE) and Western blot analysis to show levels of Acc1 oligomerisation, and crude cell fractionation followed by SDS-PAGE and Western blot to analyse protein levels and subcellular localisation of Acc1.
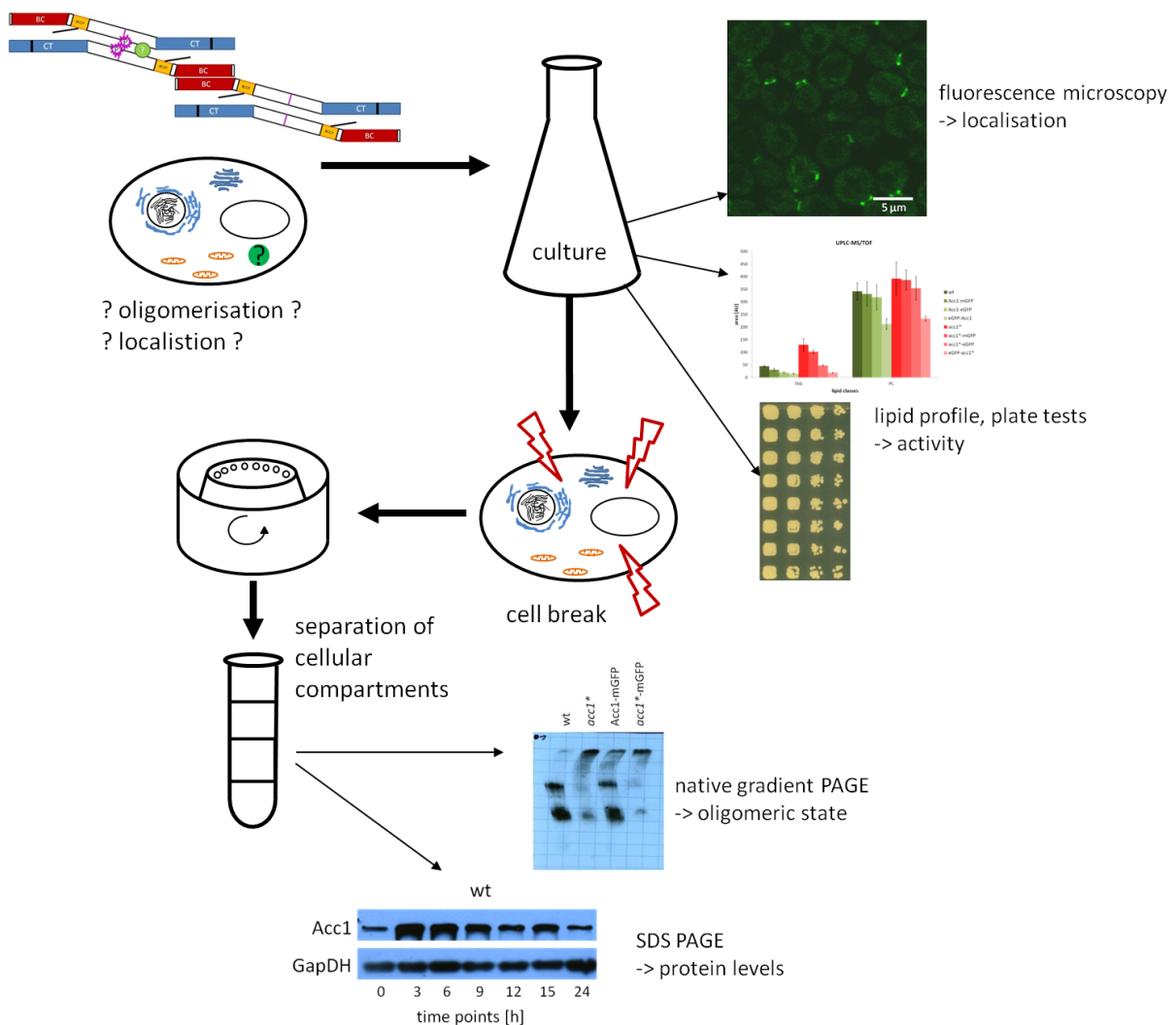
Figure 10: Work flow in this study.

2.2 Genetic modification of Acc1 for localisation and activity studies

To investigate mechanisms regulating Acc1 activity and localisation we used strains with elevated Acc1 activity and generated strains in which Acc1 is fused to a fluorescent marker, namely green fluorescent protein (GFP).

All yeast strains are congenic with BY, a derivative of S288C, and are listed in Table 1 (Materials and Methods) and Figure 11. To investigate the effects of altered Acc1 activity we used a strain with elevated Acc1 activity referred to as *acc1**. Hyperactivity of Acc1 in the *acc1** strain was achieved by a serine to alanine exchange at the position 1157, the only reported and validated phosphorylation site of yeast Acc1 [Hofbauer et al., 2014, in prep.]. Phosphorylation is known to inhibit Acc1 activity and hence a loss of the phosphorylation site leads to constantly active Acc1. To reveal differences of Acc1 localisation in living cells regarding to its activity, we tagged the native and the hyperactive enzyme at different positions with fluorescence markers, namely enhanced GFP (eGFP) and monomeric GFP (mGFP). A drawback of eGFP is its possibility to aggregate and hence to induce mislocalisation of the tagged protein. Monomeric GFP instead does not have the ability of self-aggregation and this seems to be a better solution for localisation studies (Shaner *et al.*, 2005; Remington, 2011). Besides aggregation, tagging of a protein can lead to a loss or alteration of activity due to impairment of protein interactions like dimerisation or oligomerisation, proper folding or transport. Therefore we tagged Acc1 at the C-terminus as well as at the N-terminus to identify the most wild type like form for revealing the native localisation. Tagging at the C-terminus might impair the function of the coiled coil domain and hence protein interaction or the function of the CT domain, whereas tagging at the N-terminus could prohibit activity of the BC domain or the proposed dimerisation of BC domains to form a functional enzyme oligomer.

The subsequent characterisation experiments were performed to reveal the best combination of tagging position and GFP-type for further localisation studies.
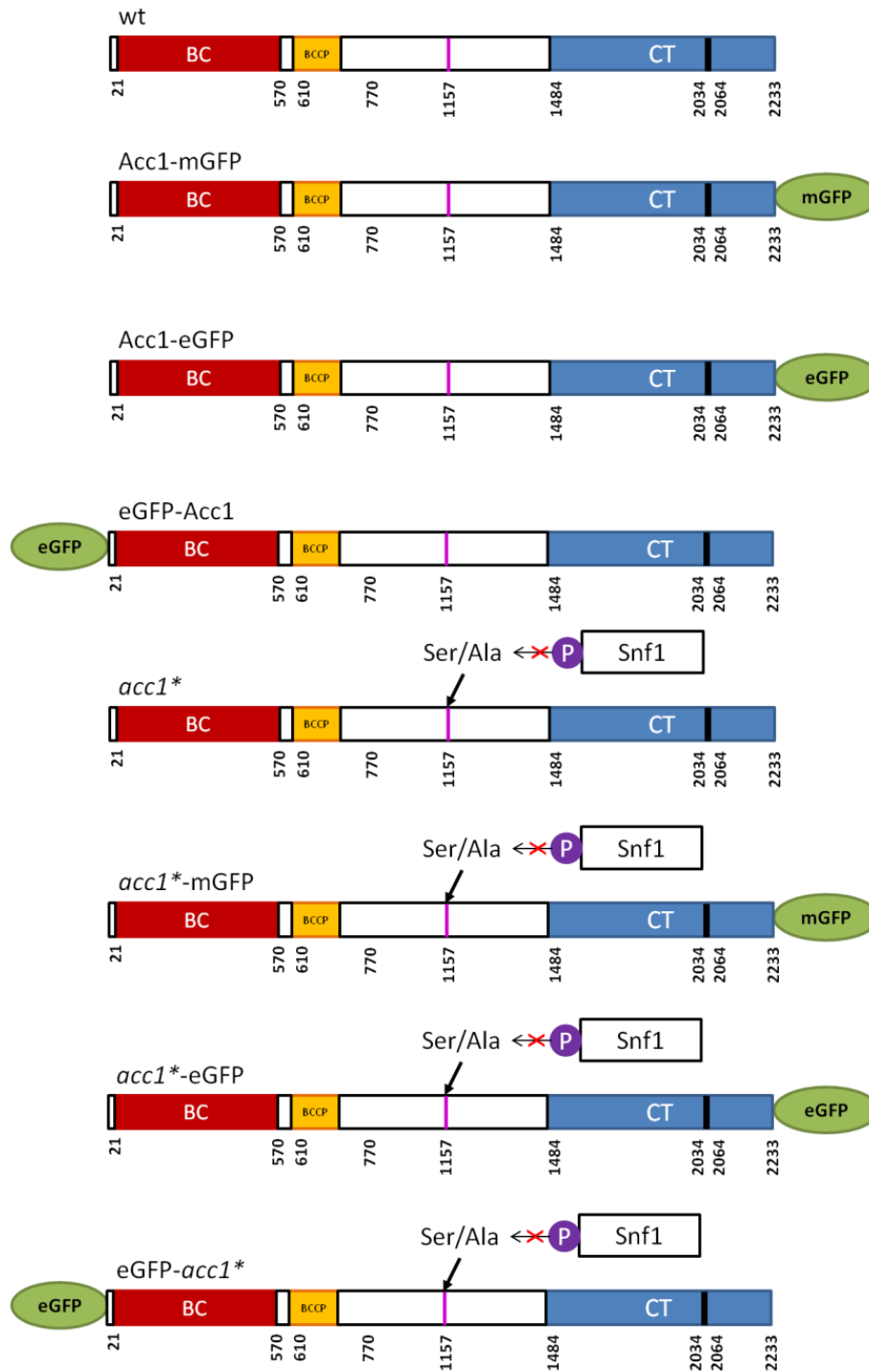
Figure 11: Acc1 modifications used in this study. The differently modified Acc1 proteins which were introduced in BY strains are schematically listed. The tag (mGFP or eGFP) is located either at the C-terminus (Acc1-mGFP, Acc1-eGFP, *acc1**mGFP and *acc1**eGFP) or at the N-terminus of Acc1 (eGFP-Acc1 and eGFP-*acc1**). The designation "*acc1**" indicates a serine to alanine exchange at position 1157 to prevent phosphorylation by Snf1, and yielding Acc1 hyperactivity.

2.3 Phenotypic characterisation

2.3.1 Viability on rich media containing Soraphen A as indirect readout for Acc1 activity

To characterise the effect of GFP tagging in our strains with respect to Acc1 activity we used Soraphen A (SorA), a known Acc1-specific allosteric inhibitor (Shen *et al.*, 2004), of different concentrations for plate test experiments. As *de novo* fatty acid synthesis is essential for cell growth and survival, the growth behaviour of cells on media containing SorA can be seen as an indirect readout of Acc1 activity.
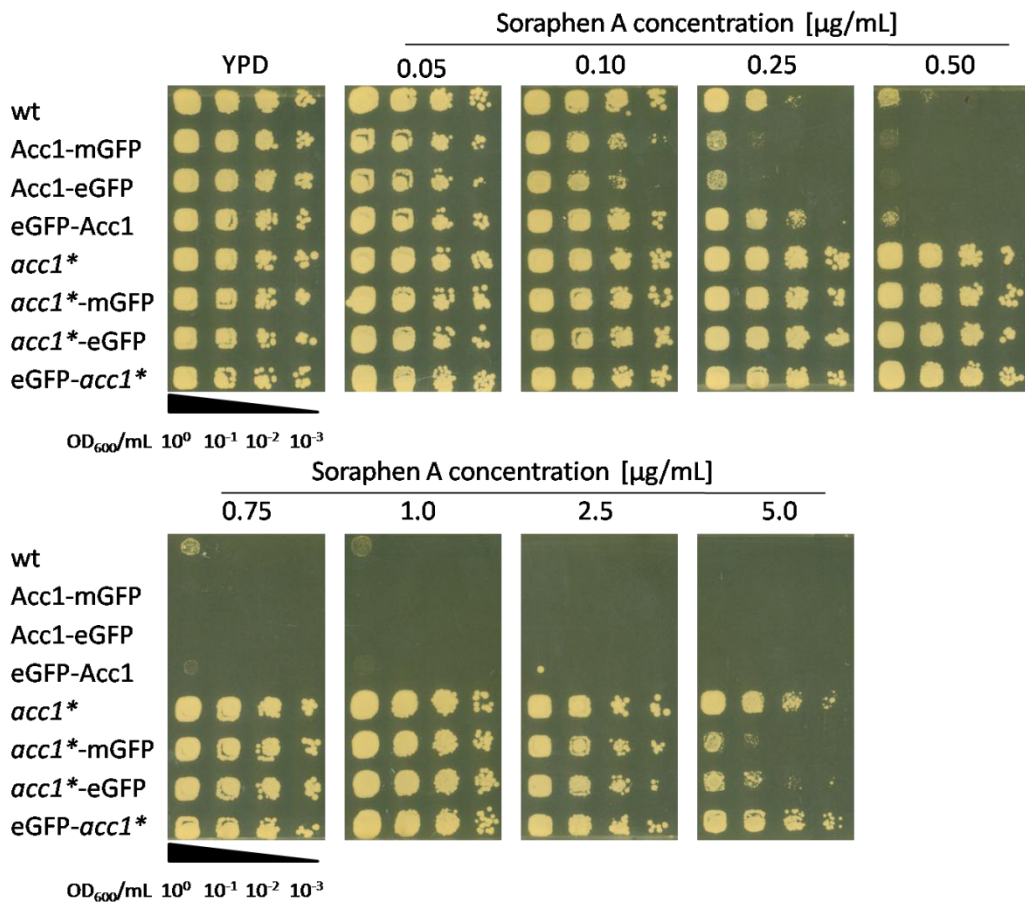
Figure 12: Soraphen A titration. This plate test shows growth of strains on media containing the Acc1 inhibitor Soraphen A and indirectly reflects Acc1 activity. Cells were grown at 30°C for 2 days on YPD containing Soraphen A as indicated.

Different resistance towards SorA was observed by comparing the wild type with the *acc1** strain. Growth of *acc1** on media containing Soraphen A was not affected up to a level of 5 µg/mL SorA, whereas wild type showed a growth defect starting at a concentration of 0.25 µg/mL SorA. This higher SorA resistance of the *acc1** strain indirectly confirms elevated Acc1 activity compared to wild type.

Tagging of Acc1 at the C-terminus affected the resistance against SorA and thereby presumably also Acc1 activity as they showed higher sensitivity to SorA treatment than the isogenic strains bearing the native Acc1 protein. This behaviour was observed in both, wild type and hyperactive Acc1 background indicating that intrinsic activity is lowered due to C-terminal GFP tagging.

In contrast to this finding, strains with N-terminally tagged Acc1 exhibited more or less the same growth like their non-tagged counterparts. This fact indicates that Acc1 activity was not impaired by the N-terminal tag, and the behaviour of these strains regarding Acc1 activity is closest to the non-tagged strains.

2.3.2 Viability on media lacking inositol to identify strains with high Acc1 activity

Inositol auxotrophy is known to be correlated to high Acc1 activity (Shirra *et al.*, 2001). Thus, media lacking inositol was used to further characterise the strains with regard to Acc1 activity.
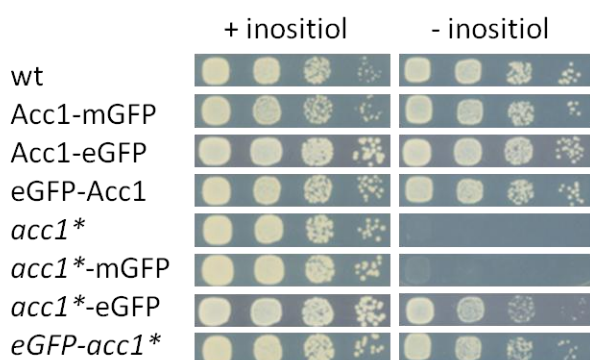
Figure 13: Inositol auxotrophy plate test. This plate test displays growth defects on media lacking inositol, an indicator for high Acc1 activity. Cells were grown at 30°C for 2 days on media with and without inositol.

All three strains bearing GFP tagged versions of the native Acc1 protein exhibited wild type-like growth on inositol free medium (Figure 13). In contrast, the *acc1** strain, as well as its mGFP tagged counterpart, showed a severe growth defect under these conditions, confirming elevated Acc1 activity in those strains. Interestingly, *acc1** strains tagged with eGFP were prototrophic for inositol, strongly indicating that their Acc1 activity is lower than in the non-tagged *acc1** and mGFP-tagged *acc1** strains.

This test for inositol-dependent growth unveiled that not the position of the tag but rather the quality of the tag (eGFP versus mGFP) affected the activity of Acc1. However, as this is contradictive to the observations from the Soraphen A plate tests, further studies had to be performed to elucidate which strains were the most relevant model strains with regard to Acc1 activity.

2.3.3 Reduced Acc1 activity results in overexpression and secretion of inositol

As shown above, highly elevated Acc1 activity renders cells auxotrophic for inositol. Conversely, studies from our group provide evidence that reduced Acc1 activity leads to overexpression and secretion of inositol (Opi⁻ phenotype; Hofbauer, Tehlivets and Kohlwein, unpublished data). By titrating Soraphen A on inositol-free media we aimed to fine-tune Acc1 activity to observe differences in inositol secretion and thus monitor Acc1 activity of the strains. To identify such an Opi⁻ phenotype we conducted a sensitive bioassay using an inositol auxotroph tester strain (AID), which was sprayed on the plates to indicate inositol secretion by a halo growth around the spotted strains.
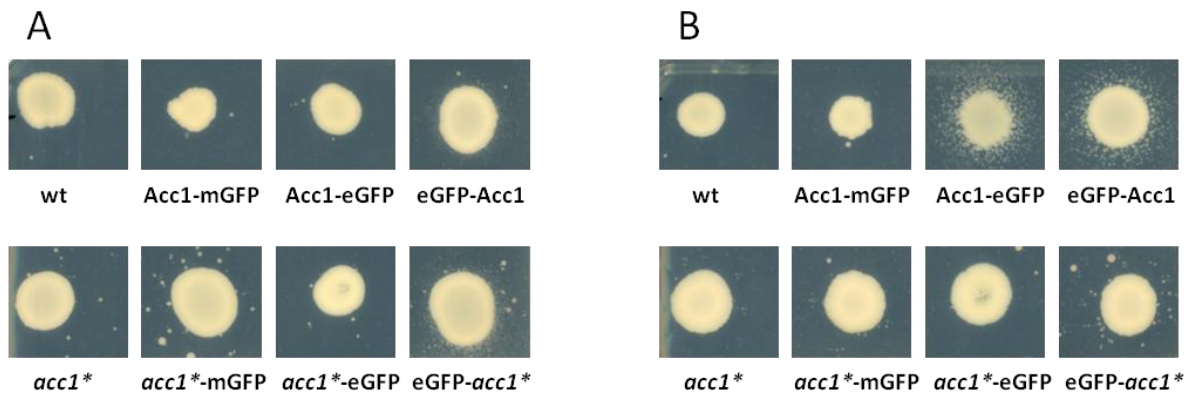
Figure 14: Opi⁻ test. Halo growth of the AID strain indicates inositol secretion of strains with reduced Acc1 activity. (A) 0.01 µg/mL SorA, grown for 4 days at 30°C, (B) 0.15 µg/mL SorA, grown for 7 days at 30°C

Strains with eGFP tagged Acc1 exhibited inositol secretion and hence a lower activity than strains with untagged or mGFP tagged Acc1. In Figure 14A the halos around the N-terminal tagged strains appear at a very low SorA concentration of 0.01 µg/mL and point out an overproduction of inositol. Stronger inositol secretion of eGFP tagged strains is induced by lowering Acc1 activity with higher SorA concentrations of 0.15 µg/mL (Figure 14B). This combination of SorA sensitivity and overproduction of inositol indicates that Acc1 activity is lowest in eGFP-Acc1 and eGFP-*acc1** followed by Acc1-eGFP. Acc1 activity of the other tested strains seems to be unaffected by SorA concentrations up to 0.3 µg/mL (data not shown).

These results further strengthen our findings with regard to inositol auxotrophy phenotypes, indicating that mGFP tagged strains exhibit Acc1 activity most closely to the physiological levels of the non-tagged strains.

2.3.4 Fluorescence microscopy displayed changes in Acc1 localisation due to tagging and activity

To reveal the localisation and possible oligomeric structures of Acc1 – as mentioned in the introduction – in wild type and the hyperactive *acc1** strain, we performed confocal laser scanning microscopy (CLSM) at distinct time points using the different GFP tagged strains to discover localisation changes depending on the tag. Simultaneously we aimed to find out whether distinct structures or a certain localisation pattern could arise by modulating Acc1 activity.
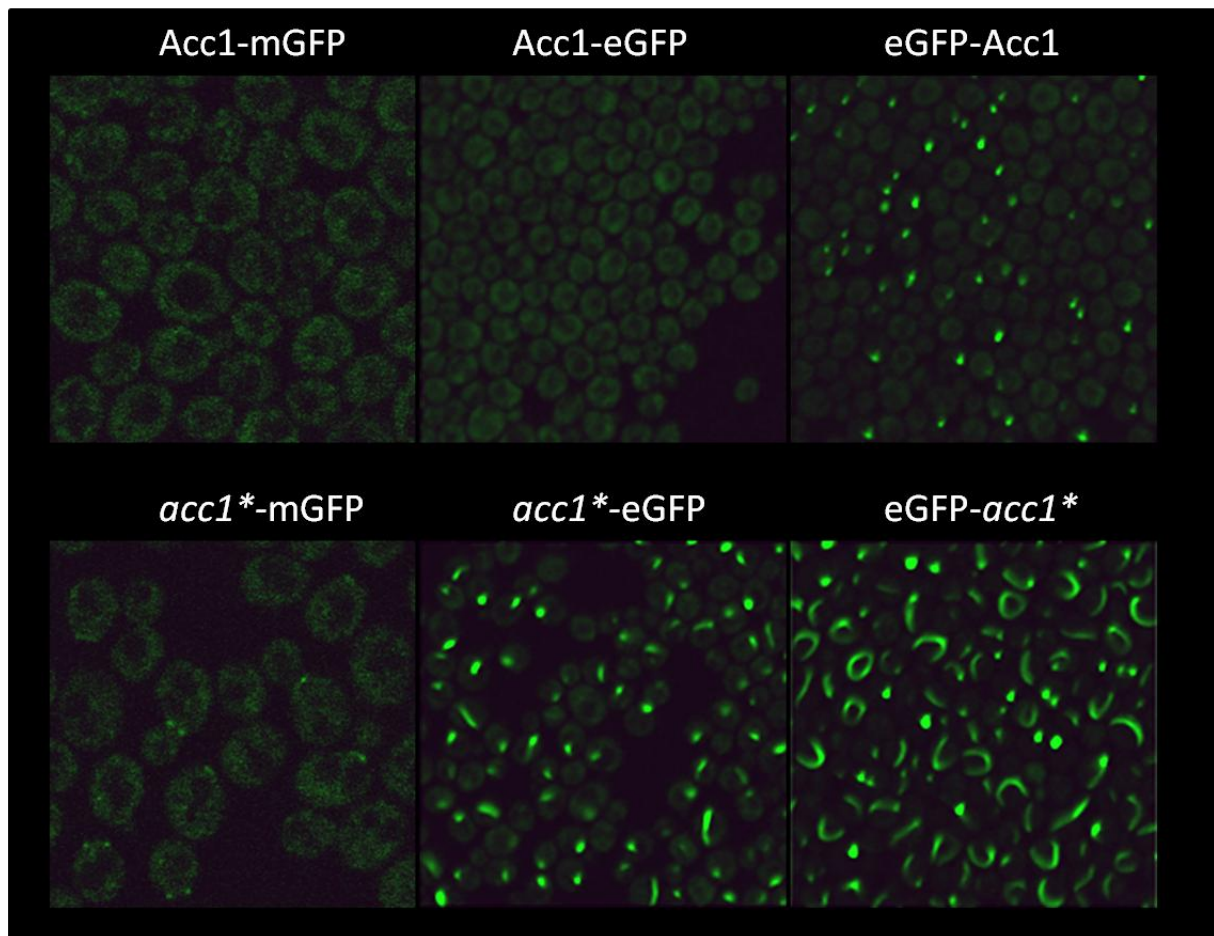
Figure 15: Confocal laser scanning microscopy of mGFP and eGFP tagged strains. The microscopy pictures revealed a heterogeneous set of Acc1 localisations, depending on the kind of tag, the position of tagging and activity of Acc1.

Fluorescence microscopy of eGFP and mGFP tagged strains during logarithmic growth phase revealed different localisation patterns of Acc1. Strains bearing Acc1-mGFP and Acc1-eGFP showed the same cytosolic localisation of Acc1. These findings suggest that in the logarithmic phase the active form of Acc1 is present in the cytosol, where *de novo* FA synthesis takes place. In contrast, eGFP-Acc1 displayed accumulation of Acc1 in dot like structures.

The comparison of this finding with the results of the C-terminally tagged Acc1-eGFP suggests that tagging of Acc1 at different positions alters its localisation. Strains bearing hyperactive Acc1 revealed yet another different localisation type, indicating that also Acc1 activity influences its localisation and/or aggregation. Interestingly, besides the cytosolic signal in the *acc1**-mGFP strain, an additional signal was observed at the bud neck. The eGFP tagged strains *acc1**-eGFP and eGFP-*acc1** displayed strong aggregation patterns reaching from dots over half-moon structures in both strains to even full rings in the N-terminally tagged strain. This shows that the use of either monomeric or enhanced GFP as tag induced changes in the localisation pattern in the Acc1 hyperactive background.

Taken together these data show that the localisation of Acc1 is affected by the type of fluorescence marker used for tagging, the position of the tag as well as by the activity of Acc1. Due to the variety of structures it is difficult to define a native localisation for Acc1. Hence we went on to further characterise the strains regarding activity using lipid composition as indirect readout of Acc1 activity.

2.3.5 Lipid profiling for further determination of Acc1 activity

Lipid analysis was used as another indirect measurement of Acc1 activity. Higher Acc1 activity results in an overproduction of malonyl-CoA which is further used for the synthesis of FA by the FAS complex. These FA in turn serve as building blocks for lipid formation. Overproduction of malonyl-CoA is problematic for the cell, therefore the excess of malonyl-CoA is shuffled into FA synthesis and elongation. The fact that FA elongation is limited to C_{26}-FA and an overflow and imbalance of FA is also harmful for the cell, FAs are finally stored in form of TAG in lipid droplets. These processes caused by higher Acc1 activity can be observed in the lipid profile in terms of higher TAG levels and a shift towards longer chain FA species.

2.3.5.1 *Thin layer chromatography (TLC) links high Acc1 activity to TAG accumulation and reduced steryl ester levels*

Pre-screening of lipid species by thin layer chromatography revealed differences of TAG and SE levels. Comparison of the isogenic strains (wild type background on the left half, hyperactive background on the right half) showed decreasing TAG levels from untagged over C-terminally mGFP and eGFP tagged to N-terminally eGFP tagged Acc1. Consistent with prior studies the hyperactive *acc1** strain showed a much higher TAG content as the wt strain (Hofbauer et al, in prep.).

The mGFP tagged strains were closest to their non tagged counterparts followed by the C-terminal eGFP-tagged strains. N terminal tagging of Acc1 with eGFP resulted in the lowest TAG levels. Notably, even the hyperactive point mutation in Acc1 failed to increase TAG amounts in these strains, which indicates a very low Acc1 activity. When comparing TAG to SE levels, a reverse correlation was observed in the distribution pattern with high TAG levels leading to low SE levels and vice versa, indicating a competition for acetyl-CoA, which is the substrate for both, FA and sterol synthesis. Using the TAG levels as readout for Acc1 activity revealed that Acc1 hyperactivity in *acc1** was most comparable to the mGFP tagged *acc1** strain.
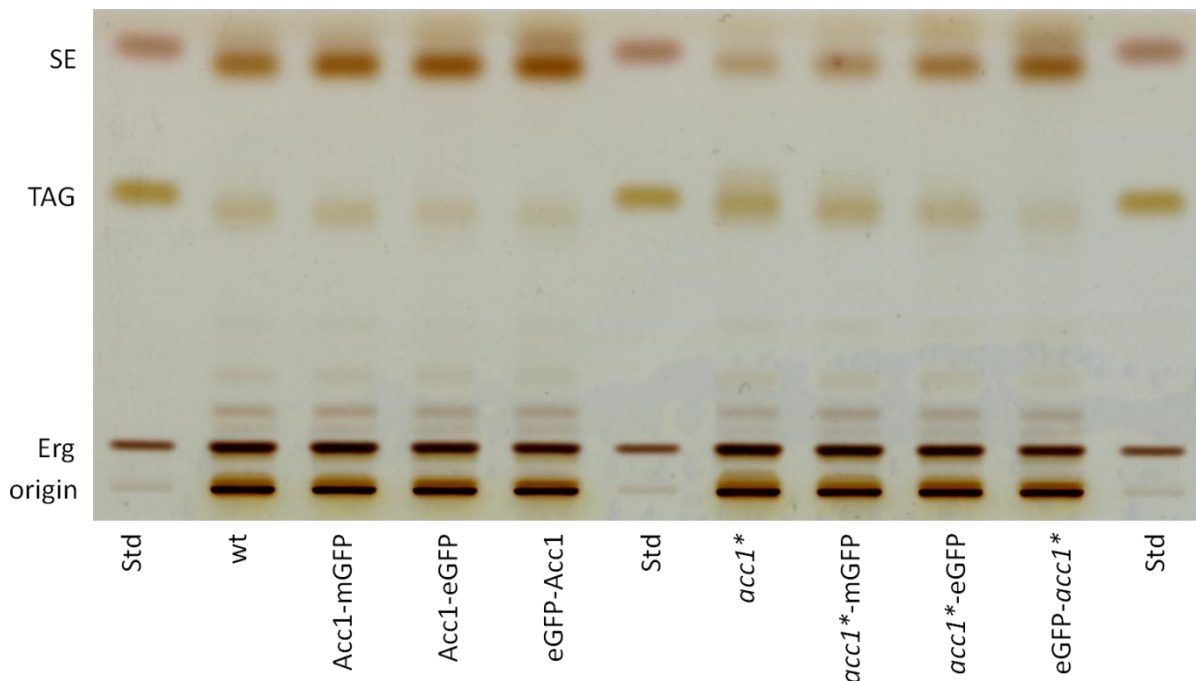
Figure 16: Thin layer chromatography. TLC analysis shows the distribution pattern of lipids in the different strains. Cells were cultivated at 30°C in liquid YPD, harvested after 5h at logarithmic growth phase and subjected to lipid extraction. Erg… ergosterol, TAG… triacylglycerol, SE… steryl ester

2.3.5.2 Lipid levels indirectly reflect Acc1 activity

Lipids were extracted and analysed by UPLC-MS/TOF (Ultra Performance Liquid Chromatography-Mass Spectroscopy with Time Of Flight detector) and HPLC-ELSD (High Performance Liquid Chromatography with Evaporative Light Scattering Detector).
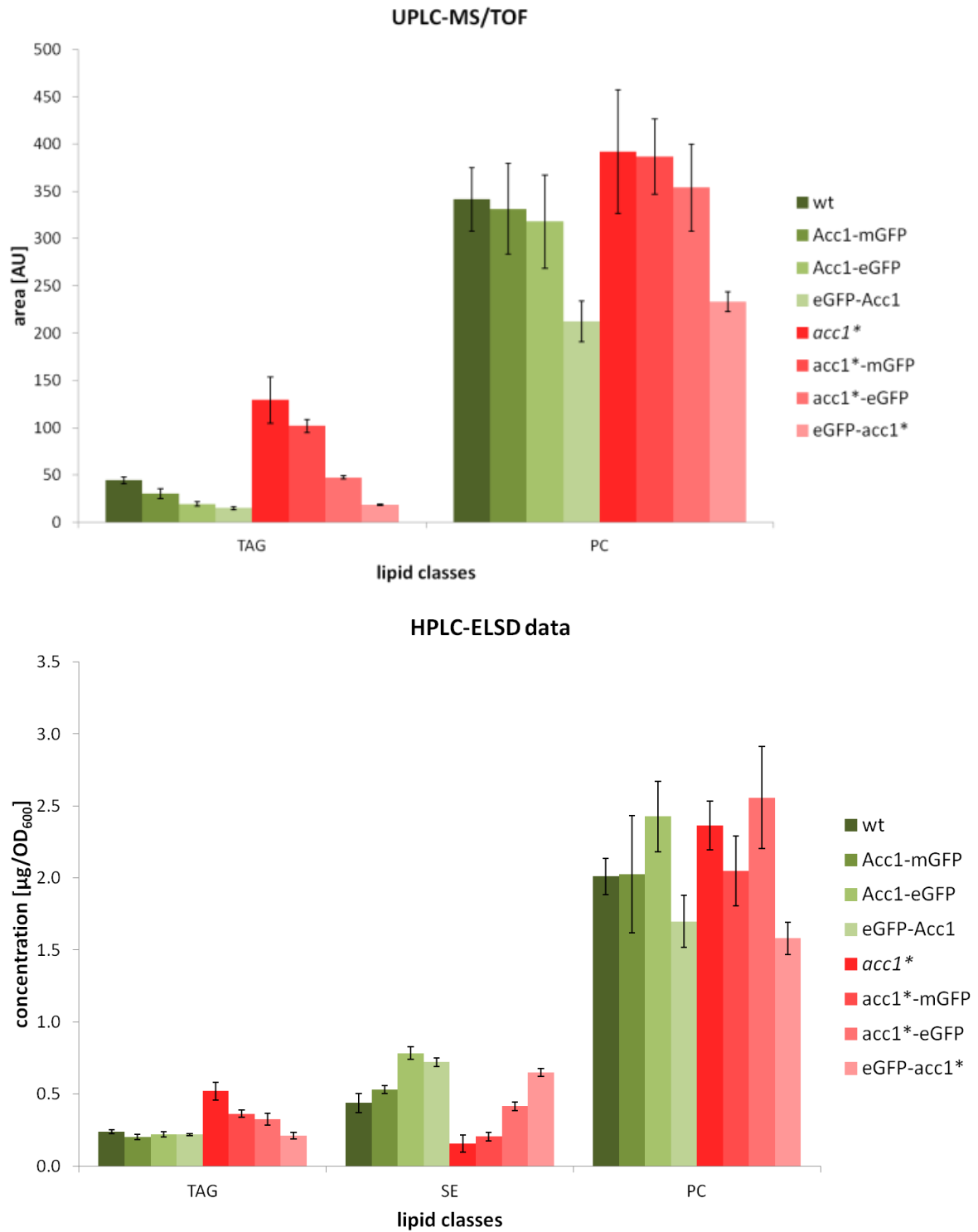
Figure 17: Lipid composition: UPLC-MS/TOF and HPLC-ELSD analysis provide the lipid composition of the different strains and indirectly reveal Acc1 activity. Cells were cultivated at 30°C in liquid YPD, harvested after 5h in the logarithmic growth phase and subjected to lipid extraction and analysis.

Comparing wild type and *acc1** with regard to the TAG levels clearly shows a significant increase of TAG in the hyperactive strain. As mentioned before, an accumulation of this storage lipid indicates that Acc1 activity is highly elevated in comparison to wild type. Especially in the hyperactive background the tagged strains showed less accumulation of TAG and exhibited the same trend towards lower TAG levels from non-tagged to N-terminally tagged Acc1 as observed on the TLC. This was also the case for the tagged strains in the wild type background, by the UPLC-MS/TOF analyses. In all cases the C-terminally mGFP tagged strains were the most comparable with the non-tagged equivalents. The *acc1**-eGFP strain displayed wild type like TAG levels in the UPLC-MS/TOF measurements. When analysed with HPLC-ELSD, the levels were slightly higher than wild type and not significantly different to *acc1**-mGFP. The most dramatic effects were observed with the N-terminally eGFP tagged strains. In the wild type background TAG levels were significantly lower than in all other strains but interestingly not even the hyperactive mutation lead to an accumulation of TAG and levels were actually below wild type in the eGFP-*acc1** strain. This is contradictive to what has been observed in SorA plate tests, but is in line with the tests for inositol auxotrophy (Figure 12 and Figure 13).

In terms of SE it appears as if Acc1 hyperactivity led to lower levels of SE. Comparing the strains among each other and also with TAG levels reveals that they exhibited a SE distribution pattern that was inverse to TAG levels, as also by TLC analysis. Again the C-terminal mGFP tagged strains were the most comparable to their non-tagged analogs.

The amount of PC was not significantly altered in all strains, except the N-terminally tagged ones. Considering also TAG levels this indicates a very low Acc1 activity in N-terminally eGFP tagged strains.

Taken together these lipid data indicate that Acc1 activity is significantly increased in the *acc1** strain and that mGFP tagged strains are the closest to untagged behaviour in terms of Acc1 activity. N-terminal tagging led to severe changes in Acc1 activity, which even suppressed the lipid phenotype of the *acc1** strain.

2.3.5.3 Species distribution in TAG and PC is dependent on Acc1 activity

Comparing the different species within TAG and PC (obtained by UPLC-MS/TOF analysis) of wild type and *acc1** revealed a distinct shift towards C18:0 and C18:1 FA containing species in the hyperactive strain. The increase of chain length was accompanied by a decrease in C16 containing species and the difference between *acc1** and wild type was most pronounced at TAG and PC species consisting just of C18 FA. This supports the assumption that the excess of malonyl-CoA in the hyperactive Acc1 strain not only increases the production of FAs, which are then channelled into TAG but is additionally used to elongate FA.

The species distribution of the mGFP tagged strains was again closest to their non-tagged equivalents. TAG and PC species shifted towards longer FA in the *acc1**-mGFP strain, displaying higher activity than in the Acc1-mGFP strain. Comparing these shifts to non tagged *acc1** indicates that Acc1 activity is slightly lower in the tagged strain, but nevertheless the results are most similar to the untagged strains. Acc1-eGFP showed a shift to longer FA in the hyperactive background as well, but not as pronounced as in the non tagged and the mGFP tagged strains.

Comparing the levels of eGFP-Acc1 and eGFP-*acc1** revealed that N-terminal tagging with eGFP led to a very slight increase in C18 containing species. Interestingly, not even the hyperactive Acc1 background was capable to provide enough Acc1 activity to achieve at least wild type lipid levels. This strongly indicates a problem of FA synthesis in this strain, independent of the observed SorA resistance. Rather, SorA resistance does not reflect the Acc1 activity but an interference of the GFP tag with the mode of inhibition of SorA on Acc1.
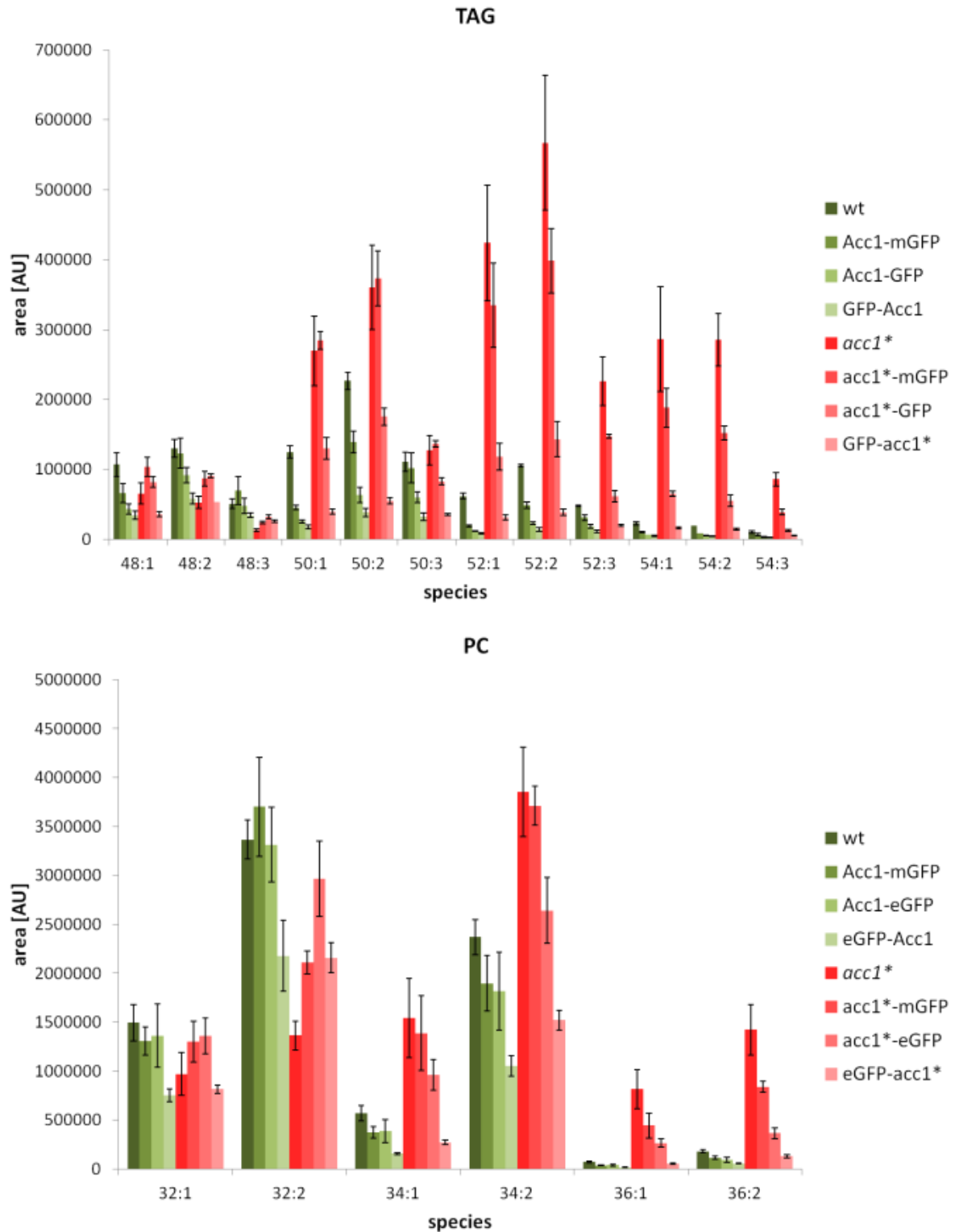
Figure 18: Lipid species: UPLC-MS/TOF analysis yields the lipid species distribution and allows conclusions about Acc1 activity. Cells were cultivated at 30°C in liquid YPD, harvested after 5h in the logarithmic growth phase and subjected to lipid extraction and analysis.

These data led to the conclusion that higher Acc1 activity results in a shift towards C18 FA containing lipid species, which is also seen in the tagged strains, but less pronounced as in the untagged ones. Acc1-mGFP and *acc1*-*mGFP again exhibited the most similar pattern compared to strains without a GFP tag.

2.3.5.4 A shift towards longer FA in the fatty acid profile points out higher Acc1 activity

Transesterification of lipids to gain fatty acid methyl esters (FAMEs) and analysis with GC-MS (and also GC-FID, data not shown) provide an overview of the whole FA profile. The obtained data confirmed the results from UPLC-MS/TOF measurements regarding FA distribution.
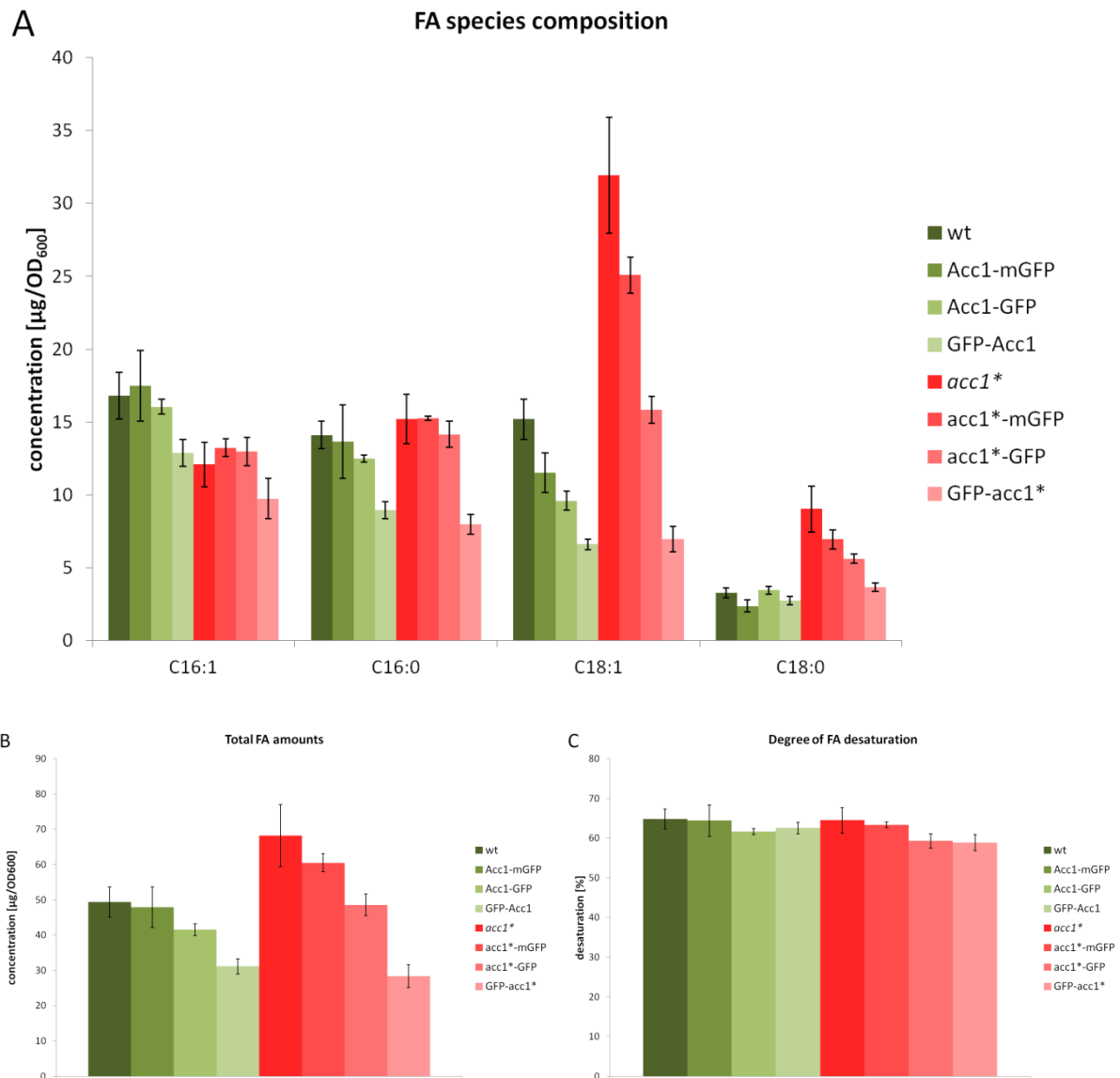
Figure 19: Fatty acid composition. The FA composition (A), total FA levels (B) and desaturation degree (C) obtained by GC-MS analysis indirectly reflects Acc1 activity. Cells were cultivated at 30°C in liquid YPD, harvested after 5h in the logarithmic growth phase and subjected to lipid extraction and analysis.

The distribution pattern of C16 FA revealed no significant changes in wild type and hyperactive mutants, perhaps slightly higher C16:1 levels in wild type. However, hyperactive Acc1 led to a shift towards C18 FA (Figure 19A), as also observed for TAG and PC species (Figure 18). This effect was very pronounced in *acc1** and stepwise disappeared in the following order: *acc1**-mGFP to *acc1**-eGFP to eGFP-*acc1**. This is also reflected by the total FA amounts of the main FA species in yeast (Figure 19B). The higher amount of C18 FA at equal C16 levels indicates increased FA production and elongation in *acc1** compared to wild type. The mGFP tagged strain also showed FA levels very similar to the non tagged equivalents, whereas C-terminally eGFP tagged strains displayed significantly lower FA levels. Consistent with other lipid data, eGFP-Acc1 and eGFP-*acc1** significantly showed the lowest FA levels. The level of desaturation remained unaltered in wild type, *acc1** and the mGFP tagged strains (Figure 19C). This demonstrates that maintaining a certain desaturation degree is substantial for cell viability under these conditions and is neither affected by increasing Acc1 activity nor by C-terminal tagging of Acc1 with mGFP.

Taken together, the lipid data revealed a dramatic accumulation of TAG and a shift towards longer FA species in the hyperactive *acc1** strain. This again confirms the higher Acc1 activity in this strain compared to wild type. Tagging of the C-terminus of Acc1 with mGFP results in slightly lowered activity but yields more similar results compared to the non tagged strains than the C-terminally eGFP tagged strains. N-terminally eGFP tagged strains show the lowest Acc1 activity and not even the S1157A mutation in Acc1 provides enough activity to yield a wild type-like FA profile when eGFP is attached to the N-terminus of the enzyme. Therefore, we concluded that the mGFP tagged strains are the most trustworthy and preferable strains for the use in further localisation experiments.

2.4 Determination of Acc1 protein levels, localisation and oligomerisation using mGFP tagging in combination with Acc1 hyperactivity

2.4.1 Growth behaviour is not changed by GFP tagging or hyperactivity of Acc1 in liquid cultures

We examined the growth behaviour of the different strains in liquid rich media to ensure that protein and lipid levels are comparable among the strains and not due to differences in growth. This is also important as time resolved experiments rely on cells being in the same growth phase at a distinct time point when compared to each other.
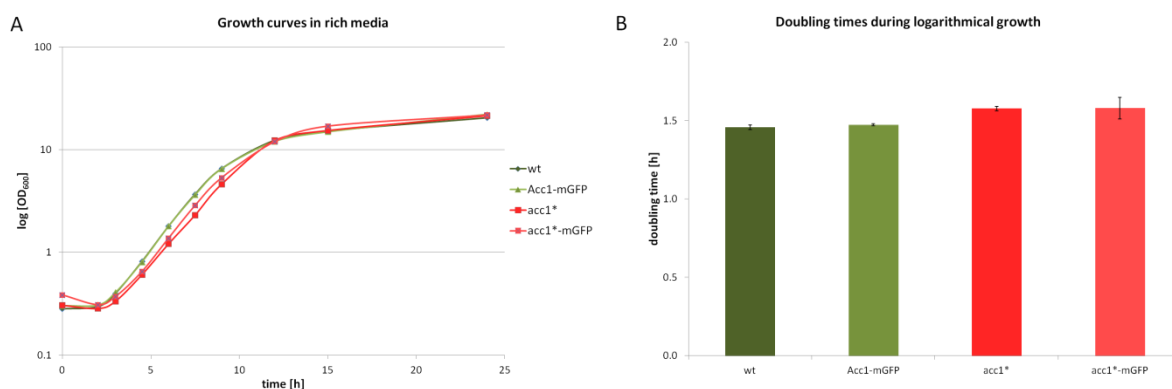
Figure 20: Growth curves and doubling times. The growth curves (A) and the calculated doubling times (B) reveal the growth behaviour of the various strains. Cells were grown at 30°C in liquid YPD and the OD_{600} measured at indicated time points.

As shown in Figure 20, growth behaviour was not significantly affected in any of the tested strains in liquid rich media as displayed by the growth curves and doubling times obtained in the logarithmical growth phase of the strains.

These results demonstrate that growth was not altered by hyperactivity or tagging of Acc1, enabling comparability of these strains in the following, more detailed investigations.

2.4.2 Acc1 protein levels are not altered by mGFP tagged or hyperactive Acc1

The clear differences obtained by lipid analysis convinced us to select the C-terminal mGFP tagged strains for further localisation studies. The next step was to investigate if Acc1 protein levels were affected by modulating activity or by tagging of the protein. To ensure that indirectly measured Acc1 activity was not simply altered due to changes in the number of Acc1 molecules present in the cell, we monitored total Acc1 protein levels by Western blot analysis during growth.
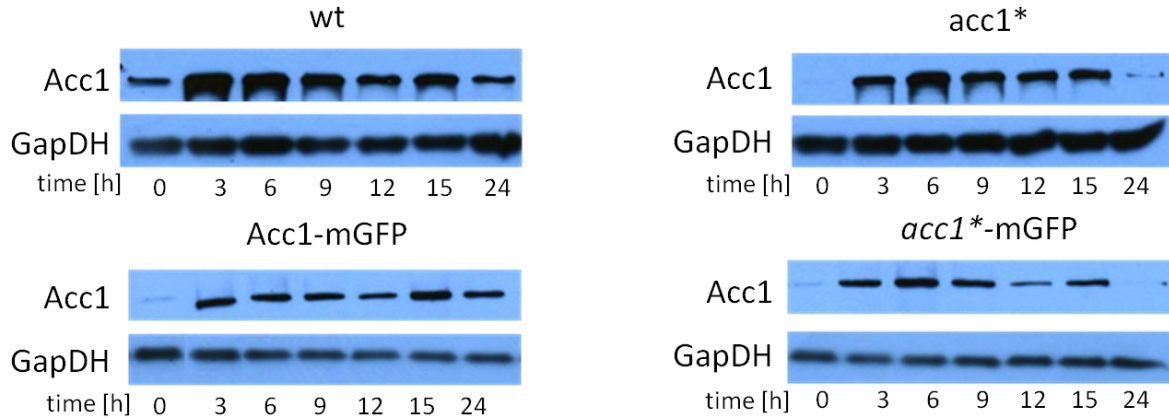
Figure 21: Total Acc1 Protein levels. Acc1 protein levels were very similar in all strains, which uncouples differences in Acc1 activity from the protein amount.

As shown in Figure 21, total protein levels displayed a similar distribution pattern during growth in all analysed strains. In stationary phase (0 hours) Acc1 was almost absent, but when cells entered logarithmic phase (3 hours), the amount of Acc1 rapidly increased. The shift from stationary to logarithmical phase appeared slightly delayed and less pronounced in the hyperactive strains. Over time, when cells became stationary, the amount of Acc1 vanished again. The time dependent Acc1 protein levels can be explained by the fact that FA synthesis is required during logarithmic growth phase but not in stationary phase.

Determination of total Acc1 protein levels revealed that neither tagging of Acc1 nor Acc1 hyperactivity changed the distribution pattern and the overall amount of Acc1 protein over time. This allowed good comparison of Acc1 activity between these strains based on the fact that differences of Acc1 activity are not caused by different protein levels.

2.4.3 mGFP tagging revealed changes in Acc1 localisation depending on Acc1 activity and growth phase of the cells

After phenotypic characterisation and selection of the C-terminally mGFP tagged strains as most comparable to non tagged ones, we went on to further investigate the localisation of Acc1. We performed microscopy studies during growth with the Acc1-mGFP and acc1*-mGFP strains to elucidate how the localisation of Acc1 was influenced by Acc1 activity and distinct growth phases of the cell.
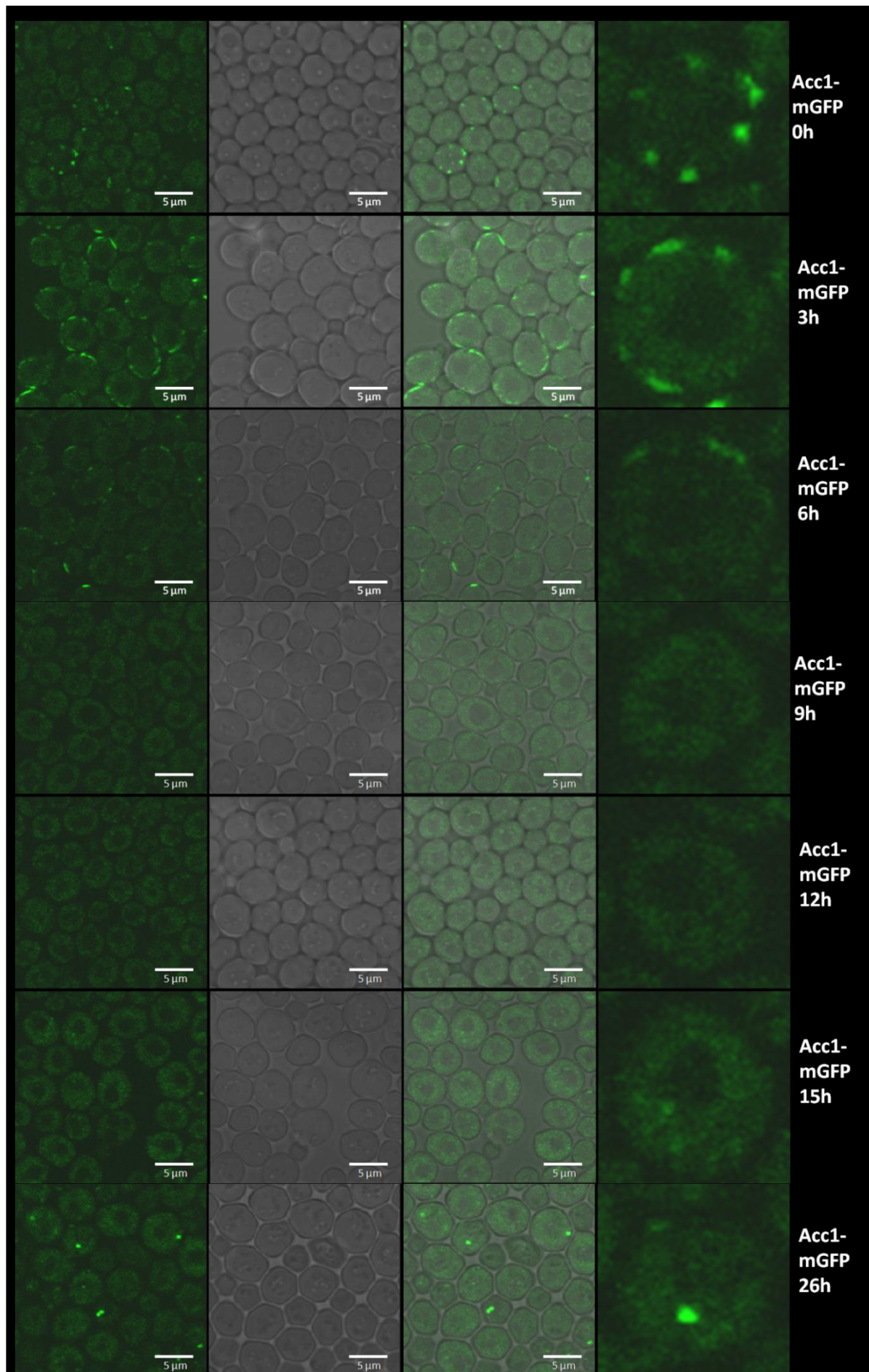
Figure 22: Fluorescence microscopy, Acc1-mGFP. This figure shows the localisation of Acc1-mGFP at different growth phases. The strains were cultivated in liquid YPD at 30°C and imaged at indicated time points.
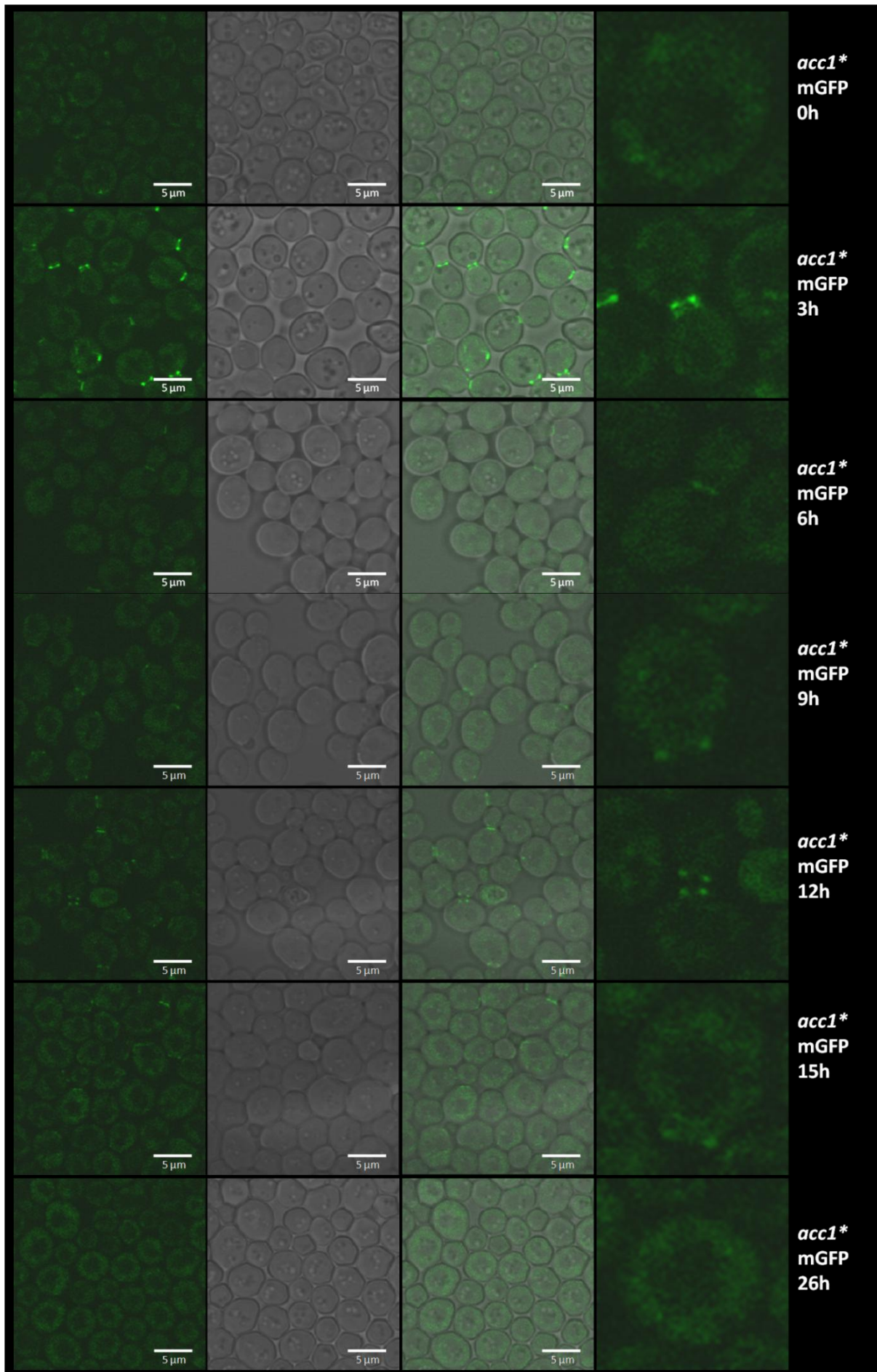
Figure 23: Fluorescence microscopy, *acc1**-mGFP. This figure shows the localisation of *acc1**-mGFP at different growth phases. The strains were cultivated in liquid YPD at 30°C and imaged at indicated time points.

Fluorescence microscopy of mGFP tagged strains further extended the localisation spectrum of Acc1 (Figure 22). Acc1-mGFP showed dot-like structures at the outer regions of the cell, perhaps associated with the plasma membrane, in stationary phase. These dot-like structures seemed to elongate and disappear when cells reached logarithmic growth (3-6 hours). In the mid logarithmic phase (9 hours) the whole Acc1-mGFP signal was found to be cytosolic. After 26 hours, when cells entered stationary phase, the dot-like structures re-appeared.

In contrast, the hyperactive *acc1**-mGFP strain showed mostly cytosolic signal in quiescent cells (Figure 23). Interestingly, as soon as cells started to divide, Acc1 was found at the bud emergence. The structures at the bud neck were very distinct and looked like two dots that are faintly connected, indicating a cut vertical ring at the plane of view. Such special structures at the bud neck are known as septin rings and proteins involved in the assembly of this rings, play a role in cell cycle progression, inhibit diffusion of large components and act as scaffold proteins (Garcia *et al.*, 2011).

Taken together these data show that the localisation of Acc1 is affected by the activity/phosphorylation of Acc1 and by the growth phase of the cell. Those findings are in accordance with *de novo* fatty acid synthesis which is known to be regulated during growth (Tehlivets *et al.*, 2007).

Due to the fact that Acc1 is not only needed for the production of LCFA but also essential for VLCFA synthesis, the enzyme may be recruited to the bud neck to provide sufficient malonyl-CoA for further FA production. These VLCFA are needed at this particular position for the formation of the new membrane and to support the membrane curvature at the budding site. As the tagging is the same in Acc1-mGFP and *acc1**-mGFP it is very likely that these differences are due to the differential activity rather than a consequence of the tag. Higher activity or the fact that *acc1** cannot be phosphorylated, clearly affect the localisation of Acc1. However, the reason why Acc1 appears at the bud neck only when the enzyme is hyperactive, remains elusive. To confirm the localisation and exclude tagging artefacts we performed indirect immunostaining coupled with fluorescence microscopy.

2.4.4 Indirect immuno-fluorescence microscopy confirmed budneck localisation of strains bearing Acc1 hyperactivity

To further confirm the previously observed localisation pattern of Acc1 and to proof that they are not an artefact of the mGFP tag, we performed immunostaining of Acc1 in wild type, *acc1**, Acc1-mGFP and *acc1**-mGFP strains. Logarithmically grown cells were fixed and treated with a monoclonal primary antibody (Ab) against Acc1 coupled with an Alexa Fluor® conjugated secondary antibody, emitting a red fluorescence signal after excitation. These treated cells were subjected to confocal laser scanning microscopy to reveal the subcellular localisation of Acc1.

In the wild type strain immunostaining of Acc1 yielded a blurry, cytosolic signal, which covered the whole cell but did not show specific structures or a distinct localisation. The Acc1-mGFP strain also exhibited a non-specific signal that confirms the cytosolic localisation of Acc1. Although the signal in the hyperactive *acc1** strain was not very defined as well, it appears to be stronger in the region between budding cells which would indicate a bud neck localisation. As the overall signal of Alexa Fluor® is very strong, it is difficult to relate this signal to a specific localisation. However, in the hyperactive mGFP tagged strain, *acc1**-mGFP, we were able to confirm the previously shown budneck localisation also by immunostaining. The *acc1**-mGFP signal clearly displayed a localisation at the bud neck but also full ring structures, which support the assumption that Acc1 associates with the septin ring. The *acc1**-mGFP signal was confirmed by binding of the specific Ab to the mGFP labelled structures in the overlay picture. A possible spectral overlap between the two fluorophores was refuted by checking for crosstalk. The strong Ab signal masks a proper identification of specific signals in the untagged strains, which is necessary to proof that the bud neck localisation is not induced by tagging of Acc1. Therefore we tested whether the secondary Ab increased the signal by unspecific binding, but the Alexa Fluor® Ab did not yield any unspecific signals (picture not shown).

Immunostaining yielded first indications for the localisation of native Acc1, but further optimisation of the immunostaining protocol is needed and in progress.
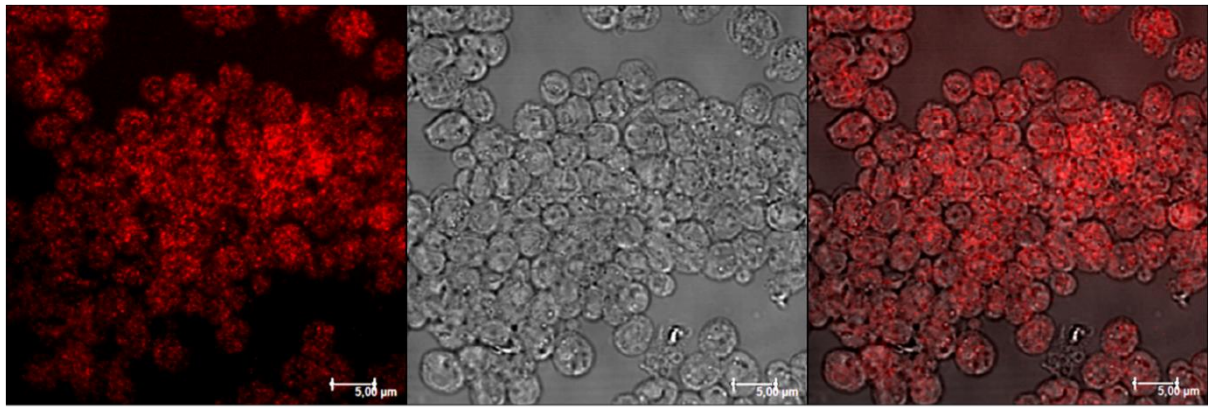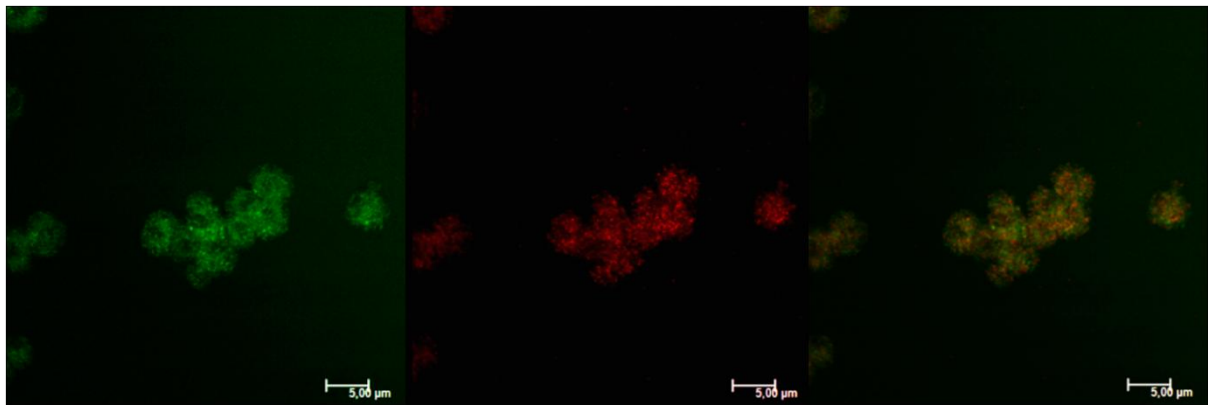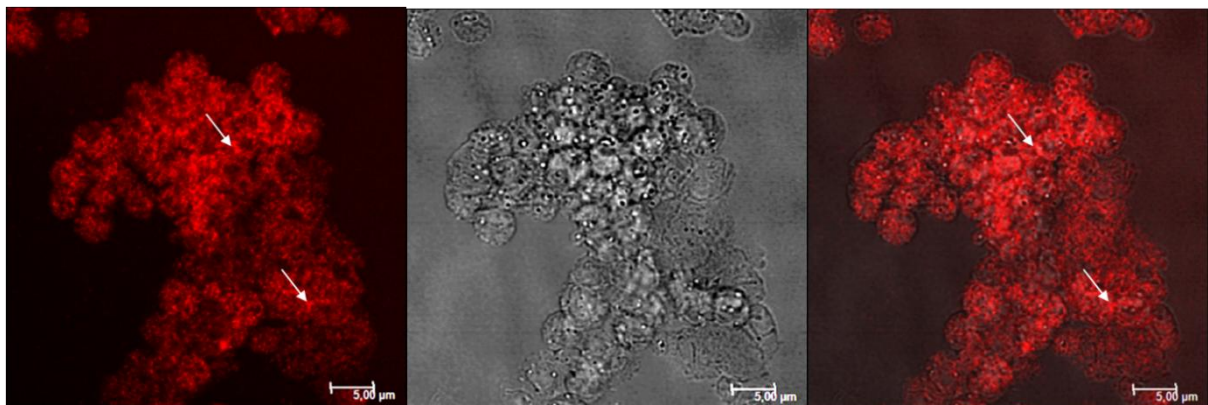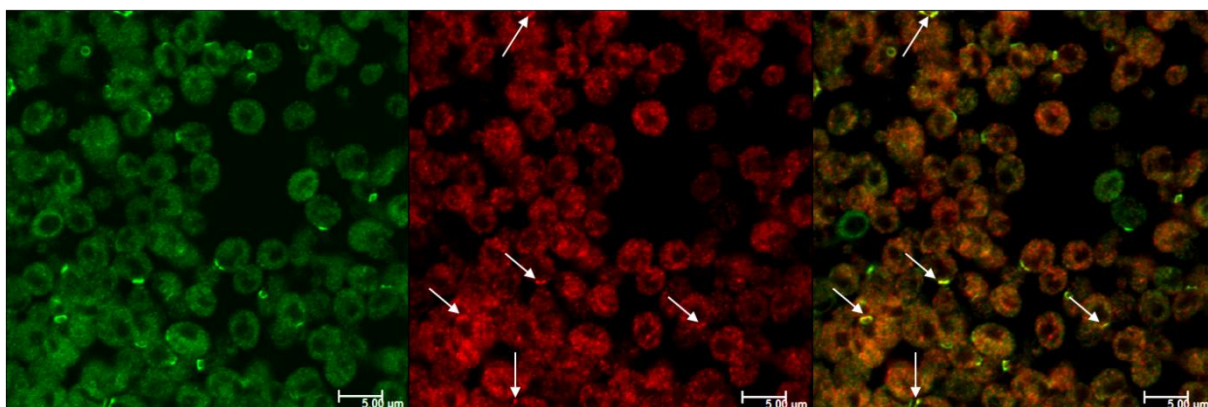
Figure 24: Immunostaining of Acc1. Immuno-fluorescence confirmed budneck localisation in the *acc1**-mGFP strain and indicates a budneck localisation of Acc1 in the *acc1** strain.

2.4.5 Further localisation studies

2.4.5.1 *acc1*-mGFP localises to the bud neck in the logarithmic growth phase*

The previously observed bud neck localisation in the *acc1**-mGFP strain raised our interest to further investigate this rather unexpected finding. Therefore, we subjected mid logarithmically growing Acc1-mGFP and *acc1**-mGFP cells to fluorescence microscopy. The results in Figure 25 confirmed the bud neck localisation of *acc1**-mGFP. However, Acc1-mGFP did not show this localisation. As mentioned before, the Acc1-mGFP signal was found to be just cytosolic during logarithmic growth.
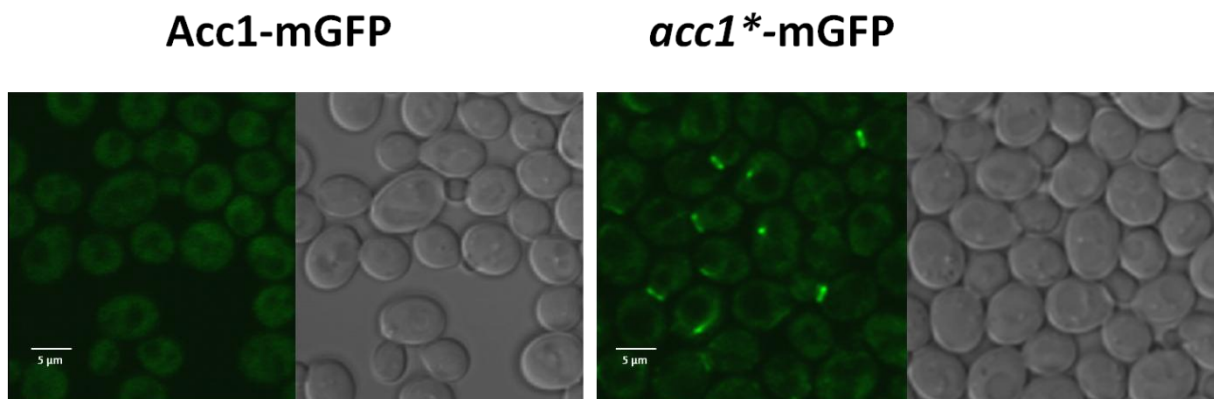
Figure 25: Fluorescence microscopy of logarithmical mGFP tagged strains. Fluorescence microscopy shows the different localisation patterns of Acc1-mGFP and *acc1**-mGFP. Cells were cultivated at 30°C in liquid YPD and imaged after 5h at logarithmical growth phase.

2.4.5.2 *No co-localisation of acc1*-mGFP and Elo3-mRFP*

As the formation of the bud neck might need very long chain fatty acids to maintain membrane curvature, we hypothesised that this is the reason why Acc1 localises to the bud neck and provides malonyl-CoA for the elongation of FA via the elongases Elo2 and Elo3. To confirm a possible interaction of *acc1**-mGFP with Elo3, we used episomally expressed red fluorescent Elo3-mRFP in a green fluorescent *acc1**-mGFP strain to visualise a possible co-localisation of Acc1 and Elo3 at the bud neck.

Figure 26 displays the bud neck localisation of *acc1**-mGFP and a localisation of Elo3-mRFP to the nuclear and peripheral ER, but there was no co-localisation of *acc1**-mGFP and Elo3-mRFP, clearly showing that they do not directly interact with each other. However, this finding does not necessarily mean that the produced malonyl-CoA is not used for LCFA elongation by Elo3.
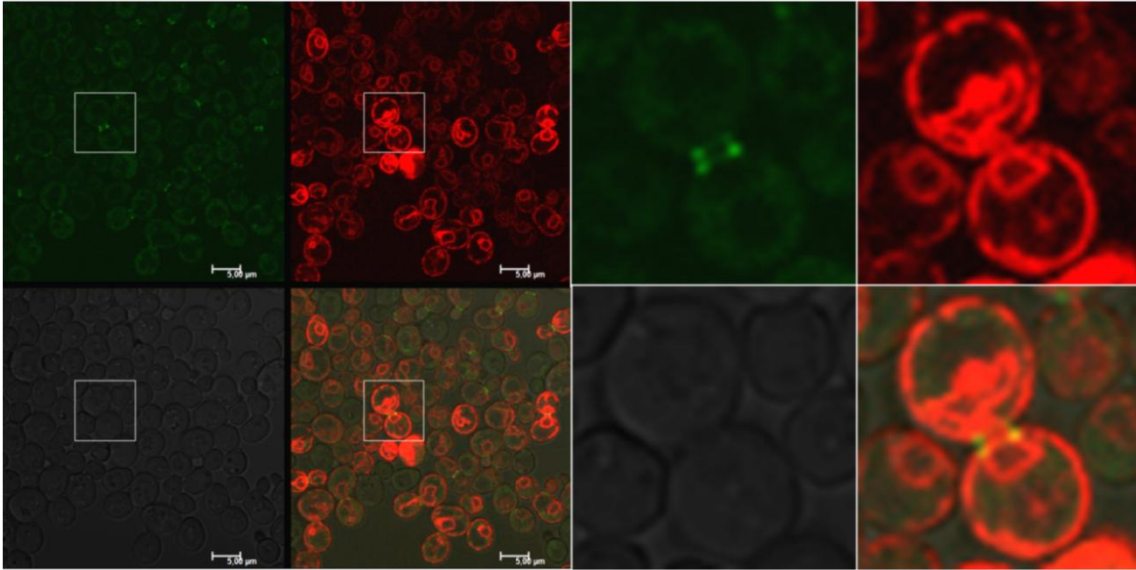
Figure 26: Fluorescence microscopy of *acc1*-*mGFP and Elo3-mRFP. This fluorescence experiment with two differentially labelled enzymes did not reveal colocalisation. Cells were cultivated at 30°C in liquid YPD and visualised after 5h in the logarithmic growth phase.

2.4.5.3 Colocalisation of acc1-mGFP & Cdc10-mRFP confirms bud neck localisation*

The assumed septin ring localisation of *acc1**-mGFP was verified using mRFP tagged Cdc10, a protein known to be involved in septin ring formation (Figure 27). The co-localisation of green *acc1**-mGFP and red Cdc10-mRFP was nicely detected by the resulting yellow colour upon merging the two fluorescence channels, strongly indicating that Acc1 is somehow recruited to the bud neck, perhaps due to the scaffolding properties of the septin ring proteins (Gladfelter *et al.*, 2001; Garcia *et al.*, 2011; Bertin *et al.*, 2012).
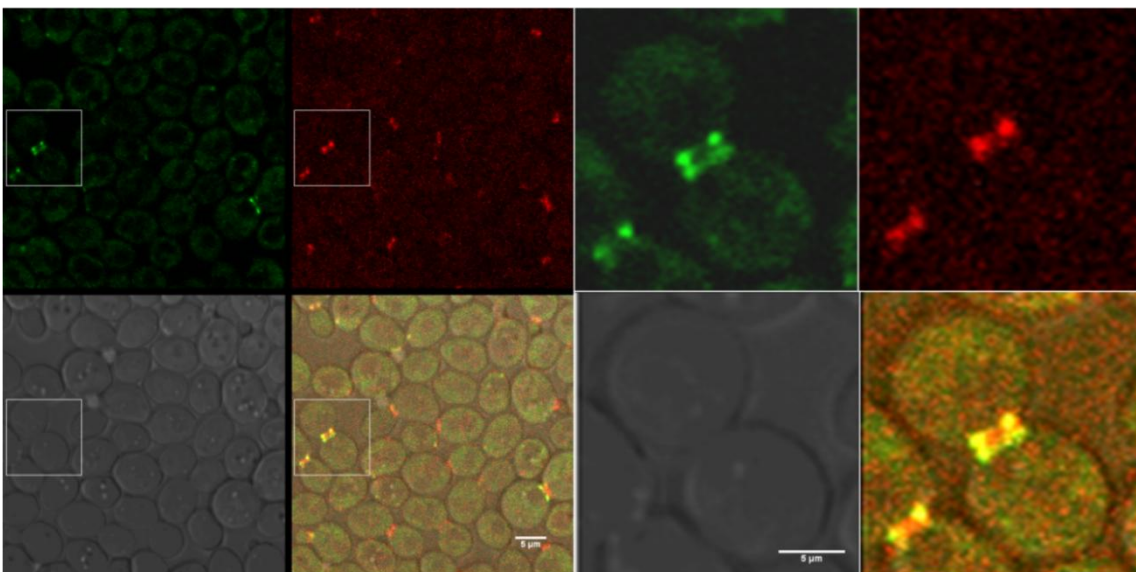
Figure 27: Fluorescence microscopy of *acc1*-*mGFP and Cdc10-mRFP. This fluorescence experiment with two differentially labelled proteins indicates colocalisation at the bud neck. Cells were cultivated at 30°C in liquid YPD and harvested after 5h in the logarithmic growth phase.

2.4.6 Organisation of Acc1 in different cellular compartments

To identify the organisation of Acc1 in different compartments of the cell, the lysate of logarithmically growing cells was subjected to differential centrifugation and the obtained fractions were applied to native gradient gel electrophoresis and western blot analysis.

2.4.6.1 Oligomeric Acc1 was only detected in the cytosolic fraction

Acc1 was only detected in the cytosolic fraction of the cell lysate (Figure 28). Both, the membrane and the pellet fraction did not exhibit any signal. This indicates that it is either difficult to extract a rather unstable, oligomeric protein like Acc1 in native form, especially from the membrane fraction, or just because there was no Acc1 present in these fractions. The cytosolic extract always yielded three individual bands, representing three different sizes of Acc1 mono/di- and homo- or hetero-oligomers, respectively. The size distribution was also different in wild type and *acc1**. Whereas in wild type the largest amount of Acc1 was in the smallest oligomeric – probably the dimeric – form, in *acc1** it was mostly present as the largest oligomeric complex. Due to the lack of high molecular weight standards in the range of 1-10 MDa, we were unable to determine the exact sizes of the detected bands.
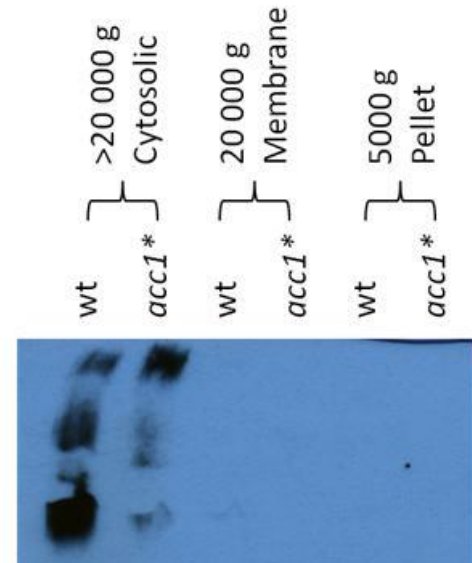
Figure 28: Native gradient gel of different fractions. Western blot analysis shows native Acc1 mono/oligomers in the cytosolic fraction. Cells were cultivated at 30°C in liquid YPD, harvested after 5h at logarithmical growth phase and disintegrated. The cell lysate was subjected to differential centrifugation and the fractions applied for native gel electrophoresis. Acc1 was visualised by western blot analysis.

2.4.6.2 Cytosolic Acc1 shows a different oligomeric distribution in wild type and acc1* background

The cytosolic fraction was further investigated with regard to these oligomeric complexes. Figure 29 displays the oligomeric patterns in the logarithmic growth phase and confirms the observed distribution before. In wild type, the majority of Acc1 was present in small and middle size oligomers whereas in *acc1**, almost all Acc1 could be found in the largest oligomeric complex. This oligomeric distribution pattern of the non tagged strains was also represented by the mGFP tagged strains which further confirmed our findings that the C-terminal mGFP tag hardly affected localisation and activity.
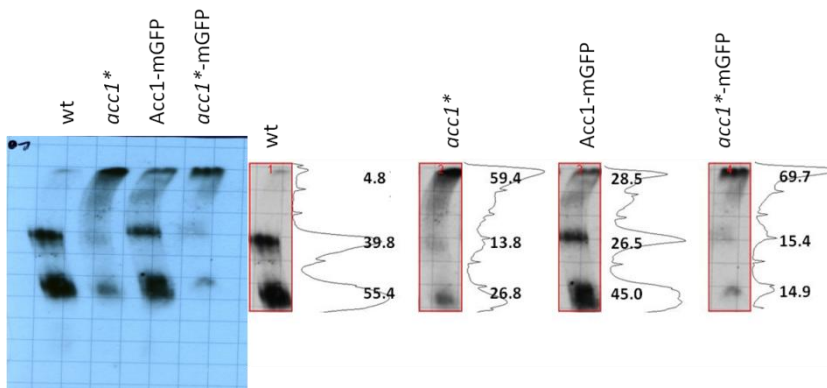
Figure 29: Native gradient gel of cytosolic fractions. This Western blot shows native Acc1 oligomers in the cytosolic fraction. Cells were cultivated at 30°C in liquid YPD, harvested after 5h in the logarithmic growth phase and disintegrated. The cell lysate was subjected to differential centrifugation and the cytosolic fraction was applied to native gradient gel electrophoresis. Acc1 was visualised by Western blot analysis.

This clearly indicates that Acc1 is present in different distinct oligomeric forms. The size of these oligomers was dependent on Acc1 activity or, conversely: the size of the oligomer determines the resulting Acc1 activity. The inability to phosphorylate Acc1 in the hyperactive *acc1** strains and the appearance of the highly oligomeric complexes in those strains somehow link the regulation via phosphorylation and oligomerisation. We hypothesise that oligomerisation leads to increased Acc1 activity and is only possible when Acc1 is dephosphorylated, proposing a combined short term regulation as an interplay of phosphorylation and oligomerisation.

2.4.6.3 Inhibition of Acc1 activity with SorA leads to increased Acc1 protein levels in wild type

Soraphen A, an Acc1-specific allosteric inhibitor, affects cell viability as shown before in the plate test experiment. To examine the influence of SorA treatment at the molecular level, wild type and *acc1** were grown in liquid rich media containing Soraphen A in different concentrations for 1.5 hours, harvested and subjected to total Acc1 protein determination via Western blot analysis.

Figure 30: Acc1 protein levels upon SorA treatment. Cells were cultivated at 30°C for 1.5 h in liquid YPD. Then they were shifted to rich media containing SorA in different concentrations, cultivated for another 1.5 h, harvested and subjected to SDS PAGE. Acc1 was visualised by Western blot analysis.

Treatment of logarithmically growing cells with SorA led to increased protein levels in wild type cells, whereas protein levels of *acc1** were not altered (Figure 30). This fits to the higher SorA resistance of *acc1** observed in the plate test experiment (Figure 12). We assume that wild type yeast cells attempt to counteract the SorA inhibited Acc1 activity by increasing the amount of Acc1 protein levels to maintain normal FA synthesis. This response upon SorA treatment is not needed in the *acc1** strain as Acc1 activity is still sufficient at the supplied SorA doses.

2.5 Summary

In conclusion, we found that tagging of Acc1 with mGFP rather than eGFP yields strains with comparable properties to strains bearing untagged Acc1. In all performed characterisation experiments, except SorA treatment on solid rich media, the mGFP tagged strains behaved very similar to their untagged counterparts.

Additionally we show that hyperactivity of Acc1 led to a bud neck localisation of the protein which indicates a possible role in cell cycle progression. A higher oligomerisation degree at mostly unaltered total Acc1 protein amounts in the *acc1** strain and the unaltered protein levels upon SorA treatment strongly indicate a connection of oligomerisation and activity of Acc1.

3 Discussion

The goal of this study was to investigate novel regulatory mechanisms that control Acc1 activity besides the known impact of Snf1 phosphorylation. Recent evidence highlighted a tertiary level of Acc1 regulation dependent on localisation and oligomerisation. Therefore, we here generated and characterised strains that were differently eGFP tagged (N- versus C-terminus) or tagged with different versions of GFP (enhanced versus monomeric GFP) in wild type and a strain bearing Acc1 hyperactivity. Careful evaluation of the results revealed strains that exhibited phenotypes closest to the non-tagged strains which were then further used to elucidate the impact of Acc1 localisation and oligomerisation on its activity level.

3.1 Phenotypic characterisation confirmed Acc1 hyperactivity in the *acc1** strain

Previous data from our lab suggested increased Acc1 activity in the point mutated *acc1** strain which lacks the Snf1 phosphorylation site in Acc1 [Hofbauer et al., 2014, in prep.]. Characterisation of this mutant strain with regard to Acc1 activity confirmed these observations. The *acc1** strain showed resistance against the allosteric Acc1-specific inhibitor Soraphen A (SorA), which is commonly used as an indirect measurement of Acc1 activity both in yeast and in mammals (Beckers *et al.*, 2007; Bozaquel-Morais *et al.*, 2010; Jump *et al.*, 2011). In consistence, this strain is auxotrophic for inositol, another known phenotype owing to high Acc1 activity (Shirra *et al.*, 2001). Preliminary data further indicated that, in turn, reduced Acc1 activity led to overproduction and sectrection of inositol (Opi$^-$ phenotype) [Hofbauer, Tehlivets and Kohlwein, unpublished]. However, the *acc1** strain did not exhibit such an Opi$^-$ phenotype upon SorA treatment which reinforces the previous observation of highly elevated Acc1 activity in this strain.

The analysis of the lipid profile also revealed a dramatic increase of TAG levels in *acc1** compared to wild type, which emphasises the high Acc1 activity of this strain. The increased TAG formation can be explained by the overproduction of *de novo* synthesised FAs when Acc1 activity is elevated. This excess of FAs is problematic for the cell and to maintain lipid homeostasis the surplus of FAs is channelled into TAG and stored in lipid droplets.

In addition to the increase of TAG levels, elongation of FA is another indication of elevated Acc1 activity. To prevent an overload of malonyl-CoA, as a consequence of highly active Acc1, the product of the Acc1 reaction is used to form longer FAs which is indicated by a shift from C16 to C18 acyl chain containing lipid species.

Taken together all these results go along with previous findings and strongly suggest high Acc1 activity when the phosphorylation site at position 1157 is point mutated and hence not susceptible to phosphorylation/inhibition by Snf1 kinase.

3.2 The position and the quality of the GFP tag affects phenotypes with respect to Acc1 activity

Characterisation of the strains bearing different tags revealed unexpected discrepancies. Despite the fact that growth was not impaired in any of the tested strains on rich media, the C-terminally tagged strains were more sensitive to SorA treatment than the N-terminally tagged strains in wild type as well as in the hyperactive Acc1 background. Surprisingly, strains with eGFP tagged Acc1, bearing the point mutation, did not exhibit inositol auxotrophy, and they showed an Opi$^-$ phenotype upon SorA treatment which is in clear contrast to the hyperactive Acc1 behaviour in the absence of a GFP tag. The Opi$^-$ phenotype was most pronounced in the N-terminally eGFP tagged strains which is contradictive to the growth on rich media containing SorA. One possible explanation would be that the N-terminal tag shields the BC domain dimerisation from SorA but additionally prohibits a proper oligomerisation of Acc1 thus yielding strains which are SorA resistant and have low Acc1 activity at the same time (causing inositol prototrophy). The Opi$^-$ phenotype and inositol prototrophy of C-terminally eGFP tagged strains is harder to explain. A possible masking of the coiled coil domain by the GFP tag and thereby inhibiting essential protein interactions is unlikely because mGFP tagging at the C-terminus of Acc1 did not yield the same phenotypes. Therefore it appears rather a matter of the quality of the tag - as eGFP tends to self aggregation - than the position, which causes lower Acc1 activity and hence Opi$^-$ phenotypes and inositol prototrophy.

The visualisation of Acc1 in these strains also displayed a wide range of different localisation patterns in the logarithmic growth phase. The eGFP tagged strains showed aggregation of Acc1 whereas the mGFP tagged strains exhibited a cytosolic and a bud neck signal respectively, depending on Acc1 activity.

As eGFP is capable to form homodimers, these aggregation structures might be tagging artifacts, which do not represent the native localisation behaviour of Acc1, presumably also affecting Acc1 activity as discussed above. Tagging with mGFP prevents such tag dependent dimerisation and, thus, more likely exhibits authentic Acc1 localisation.

Finally, lipid analysis was taken as the most reliable readout to indirectly determine Acc1 in vivo activity. Comparing the tagged strains with their non tagged counterparts revealed that the mGFP tagging reflects the highest similarity to wild type and *acc1**. The shifts towards longer FA and TAG accumulation are in accordance with SorA, Ino$^-$ and Opi$^-$ phenotypes and suggest that mGFP tagged Acc1 has a slightly reduced activity, which is also reflected by the higher SorA sensitivity, but eventually it is much closer to native Acc1 behaviour than C-terminal and N-terminal eGFP tagging of Acc1. The observed changes in TAG/SE ratios can be explained by a competitive mechanism of FA and ergosterol synthesis, which are both using acetyl-CoA and NADPH from the same substrate pool.

All experiments which were performed to characterise the phenotypes led to the final conclusion that C-terminal mGFP tagging of Acc1 yields the closest to wild type fusion protein for a further elucidation of Acc1 localisation and oligomerisation.

3.3 Acc1 localisation is dependent on growth phase and activity

Confocal laser scanning microscopy clearly displayed growth phase dependence of Acc1 localisation in the mGFP tagged strains. Native Acc1 localisation changes due to different requirements in the course of distinct growth phases. In stationary phase, when Acc1 activity is not needed and *de novo* FA synthesis is switched off, Acc1 localised to dot-like structures at the cell periphery. These dots might represent an Acc1 storage compartment for reasons of energy saving and a fast response to achieve logarithmic growth after stationary phase. When the cells enter the logarithmic phase, *de novo* FA synthesis is needed to supply the growing and dividing cells with FAs. This is indicated by the disintegration of the dot-like structures during early phases of logarithmic growth and an increase in cytosolic Acc1 signal. As mentioned before, *de novo* FA synthesis is a cytosolic process and hence localisation of Acc1 to the cytosol is required for the formation of malonyl-CoA, the substrate of the FAS complex.

Appearance of the dot-like Acc1 localisation when the cells enter stationary phase again, strengthens the assumption that these structures represent storage compartments.

No such storage structures were detected in the hyperactive mutant, which can be a consequence of the already very high Acc1 activity. The cell does not need to store Acc1 protein to support sufficient growth at the beginning of the logarithmic phase when enough activity is provided by a few Acc1 molecules. These microscopic observations were supported by total Acc1 protein determinations over time (2.4.2). Comparing strains bearing hyperactive Acc1 to wild type revealed very low levels of hyperactive Acc1 in stationary phase. This indicates that the cell does not store highly active Acc1 during times when *de novo* FA synthesis is not needed and a sufficient response to logarithmic growth is carried out by just a few newly synthesised or either still present hyperactive Acc1 molecules.

However, when cells bearing hyperactive Acc1 enter logarithmic growth and start to divide, Acc1 localises to the emerging site of budding cells. In the Acc1-mGFP strain this budneck localisation is not detectable, however, as the tag is the same in both strains, mGFP-induced mislocalisation is not very likely. A possible explanation is the formation of bigger oligomers when the Acc1 phosphorylation site is missing. We showed that a point mutation at position 1157 of Acc1, preventing phosphorylation as the only difference to wild type Acc1, causes a notable increase in oligomerisation (Figure 29) and hence activity. These oligomers are easier to detect and we belive that Acc1 might also be at the bud neck in the Acc1-mGFP strain, but not in such a highly oligomeric form that causes this distinct ring structure. There is some evidence that Acc1 was also found to be involved in spindle pole formation (Vazquez-Martin *et al.*, 2013) and that a loss of Acc1 activity results in G2/M arrest (Al-Feel *et al.*, 2003). This supports the observed bud-neck localisation of Acc1 and indicates that Acc1 has a function in cell cycle progression. We further suggest that Acc1 is needed at the budneck to provide malonyl-CoA for the synthesis of essential VLCFA (Hasslacher *et al.*, 1993; Shirra *et al.*, 2001; Tehlivets *et al.*, 2007) to sustain the extreme membrane curvature at this position. We tried to show an interaction of Acc1 with Elo3-mRFP, an enzyme involved in the elongation process, but no co-localisation of these two enzymes was observed.

However, this does not mean that the malonyl-CoA produced by Acc1 is not used by Elo3-mRFP and a localisation close to it might be needed to provide malonyl-CoA for FA elongation before it is consumed by the FAS complex for LCFA synthesis or decarboxylated by malonyl-CoA decarboxylase (Cheng *et al.*, 2006). Co-localisation of *acc1**-mGFP with Cdc10-mRFP confirmed the bud neck localisation and indicates interaction of Acc1 with the septin ring. Proteins involved in septin ring formation are known to act as scaffolding proteins and play an important role during cell division (Gladfelter *et al.*, 2001; Garcia *et al.*, 2011), which suggests that Acc1 is recruited to the septin ring for cell cycle reasons. It has also been proposed that septins mediate membrane curvature by deforming the membrane or recruiting proteins to carry out changes in membrane curvature at specific positions (Warenda and Konopka, 2002; Tanaka-Takiguchi *et al.*, 2009). This reinforces the hypothesis that Acc1 plays a role in mediating the membrane composition by providing malonyl-CoA for VLCFA synthesis and hence cell cycle progression.

To further confirm the observed bud neck localisation of hyperactive Acc1 and to prove that this particular signal is not an artefact induced by mGFP tagging, we performed immuno labelling of Acc1. The immuno staining of Acc1 indeed indicated that the localisation of Acc1 is not altered by tagging. Additionally, the fact that Acc1-mGFP, bearing the same tag as *acc1**-mGFP, did not show an identical bud neck signal strengthens the assumption that the localisation is not induced by the mGFP tag. However, the immuno stain process has definitely to be improved to yield unambiguous results.

3.4 Oligomerisation is a short term regulation mechanism of Acc1 activity

Neither point mutagenesis of Acc1 nor C-terminal tagging with mGFP altered the growth behaviour of strains. The very slightly higher doubling times of strains bearing hyperactive Acc1 cannot be considered as a significant growth defect. This renders these strains and hence lipid data, protein levels and microscopy comparable, and differences can directly be related to changes in Acc1 activity.

To show that there is an additional step of regulation independent of protein amount, we had to ensure that differences of indirectly measured Acc1 activity were not simply due to differences in the quantity of Acc1 protein.

The measured total Acc1 protein amounts in the different strains at distinct time points revealed no significant changes that explain the dramatic increase of Acc1 activity in *acc1** strains. The long term regulation on the transcriptional level did not respond to the elevated Acc1 activity within the measured timescale, which is in accordance with the half life of ACC1 of around 1-3 days (Munday, 2002).

This discloses an additional regulation step beside, or along, with the known transcriptional or posttranslational regulation mechanisms. We propose that this third level of regulation is achieved by oligomerisation of Acc1.

3.4.1 The lack of the Acc1 phosphorylation site at serine 1157 allows higher oligomeric structures and thus elevated activity

The only difference between wild type and the hyperactive Acc1 enzyme is a serine to alanine exchange at position 1157, the only known phosphorylation site of yeast Acc1. However, the lack of this phosphorylation site revealed tremendous effects on the activity as well as on the oligomerisation pattern of the enzyme. The highly elevated activity of hyperactive Acc1 was already extensively discussed above. Interestingly, the increase in Acc1 activity was accompanied by a shift towards higher oligomeric structures, which links enzymatic activity of Acc1 to oligomerisation. Native gel analysis revealed a remarkable difference between wild type and hyperactive strains regarding their Acc1 oligomer distribution. In strains bearing hyperactive Acc1, the protein was mainly present in the highest oligomeric form, whereas wild type Acc1 exhibited mostly smaller oligomers. This is in accordance with the observation that in the native state around 60% of all Acc1 is phosphorylated [Hofbauer et al., 2014, in prep.] and suggests that phosphorylation affects oligomerisation. Additionally, the oligomers appeared as distinct bands, showing almost no smear which indicates that the oligomers consisted of distinct sizes, bearing a certain number of Acc1 building blocks.

From these data we concluded that phosphorylation has an impact on the oligomerisation of Acc1, and the formation of oligomers is required to increase Acc1 activity. The interplay of phosphorylation and oligomerisation was already proposed for mammalian Acc1 by Borthwick et al. (Borthwick *et al.*, 1987). Kim and co-workers identified a protein – MIG12 - that increases oligomerisation of mammalian Acc1 while the phosphorylation level remains unaltered (Kim *et al.*, 2010).

We searched for homologous proteins in yeast and came up with Dsn1, an essential component of the MIND kinetochore complex, but co-localisation studies using Dsn1-mRFP in strains with mGFP tagged Acc1 did not reveal co-localisation. To find possible interaction partners of oligomeric complexes we subjected the native first dimension gel to a denaturing second dimension SDS-PAGE (Fiala *et al.*, 2011). However, due to low Acc1 protein levels we were not able to visualize protein signals. Enrichment of endogenously expressed Acc1 using lyophilisation, sucrose gradient centrifugation, size exclusion chromatography, avidin column purification and size exclusion centrifugation did not yield stable native Acc1 complexes. To prove that the complexes on the native gel represent oligomeric Acc1, we tried to treat growing cells, as well as cell extracts, with SorA to induce degradation of the oligomers to yield smaller aggregates. Unfortunately, methanol that was used as solvent of SorA, led to aggregation effects, and no satisfying results were obtained. By combining our results with already existing ideas and findings we came up with a model shown in Figure 31.

Figure 31: Proposed model for the regulation of Acc1 activity by oligomerisation. This model includes the activation of Acc1 through dimerisation at the BC domain and the counteracting SorA binding. Oligomerisation takes place at the domain between BCCP and CT, maybe mediated through proteins like the mammalian MIG12, and enhances Acc1 activity. Phosphorylation by Snf1 seems to influence oligomerisation by preventing the interaction of dimers through electrostatic repulsion.

This model includes the activation of Acc1 through dimerisation at the BC domain and the inhibitory effect of SorA by binding to the BC domain and prohibiting the formation of Acc1 dimers (Shen *et al.*, 2004; Tong, 2005). We suggest that oligomeristion is achieved by interaction of a domain with unknown function, located between the BCCP and the CT domain, linking two dimeric Acc1 and thereby increasing Acc1 activity by forming a tetramer in which CT and BC domains are placed opposite to each other.

Continuing this reaction with other dimers yields highly active, oligomeric structures. However, we have not identified in yeast so far a protein like the mammalian MIG12 that mediates Acc1 oligomerisation. Figure 31 shows that the phosphorylation sites of the putative oligomerisation "domain" are located closely to each other in our model. We propose that phosphorylation leads to negative charges in close proximity that will ultimately cause repulsion of the subunits and hence prohibit oligomerisation and high Acc1 activity. The coiled coil domain located at the C-terminus might provide an interaction site for the recruitment of yet unknown scaffolding proteins for Acc1 regulation or for the recruitment of Acc1 itself to the septin ring as discussed above. The fact that some septin proteins also exhibit a coiled coil domain which is not used for the interaction of the septin proteins among each other (Longtine *et al.*, 1996) supports this hypothesis.

3.5 Outlook

As there as the next step a suitable (non-radioactive) *in vitro* activity assay has to be implemented, to prove Acc1 activity and characterise the enzyme with regard to Michaelis-Menten kinetics. It is also necessary to show which oligomeric form of Acc1 – most likely the largest - harbours the activity. However, in vitro assays are problematic because cell fractionation can alter the oligomeric state of the enzyme.

Further investigations on the effects of hyperactive Acc1 should include the consumers of the product of the Acc1 reaction malonyl-CoA, namely the FAS complex and the elongases, to investigate a possible response to elevated levels of this intermediate. In one scenario the elevated malonyl-CoA levels might cause response by which the cell tries to get rid of the malonyl-CoA overflow by elevating the levels/activity of FAS and the elongases. Another possibility is that the cell tries to prevent an overflow of FA by downregulation of FAS or elongase amount/activity. Such scenarios might also include a localisational change of the involved enzymes. Vice versa we would expect a reduction of Acc1 activtiy when the FAS complex or elongases are knocked out. Hence we should observe smaller oligomers and higher levels of phosphorylation. Perhaps also localisation changes of Acc1 can be induced in such knockout strains. These findings should ideally also be translated and confirmed in mammalian cell lines to further highlight their importance with respect to regulation of a key player in lipid metabolism, Acc1.

4 Materials and methods

4.1 Strains and Media

S. cerevisiae strains used in this study are congenic with BY, a derivative of S288C, and are listed in Table 1.

Table 1. Strains used in this study

Strain	Genotype	Source
wild type	*MATa his3Δ1 leu2Δ0 lys2Δ0 met15Δ0 ura3Δ0*	Laboratory strain
acc1*	*MATa ACC1^{S1157A} his3Δ1 leu2Δ0 lys2Δ0 ura3Δ0*	This study
Acc1-mGFP	*MATa ACC1-mGFP-NATMX his3Δ1 leu2Δ0 lys2Δ0 met15Δ0 ura3Δ0*	This study
acc1*-mGFP	*MATa ACC1^{S1157A}-mGFP-NATMX his3Δ1 leu2Δ0 lys2Δ0 ura3Δ0*	This study
Acc1-eGFP	*MATa ACC1-GFP-HIS3MX6 his3Δ1 leu2Δ0 met15Δ0 ura3Δ0*	Open Biosystems
acc1*-eGFP	*MATa ACC1^{S1157A}-GFP-HIS3MX6 his3Δ1 leu2Δ0 met15Δ0 ura3Δ0*	This study
eGFP-Acc1	*MATα GFP-HIS3MX6-ACC1 his3Δ1 leu2Δ0*	Thomas Kroneis
eGFP-*acc1**	*MATα GFP-HIS3MX6-ACC1^{S1157A} his3Δ1 leu2Δ0 ura3Δ0*	This study

4.2 Culture conditions and calculation of doubling times
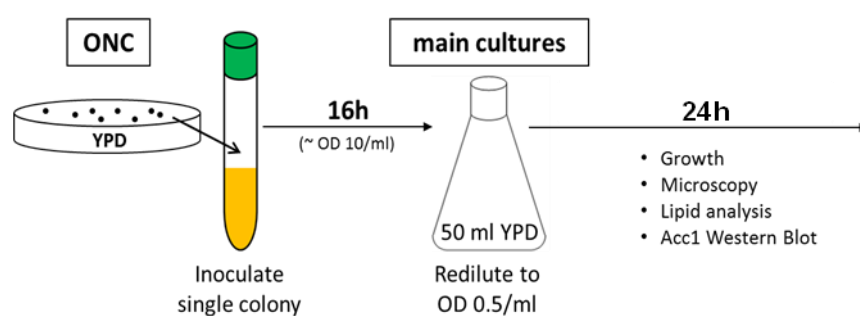
Figure 32: Cultivation of all strains used for analysis

Cells were cultured on a rotary shaker at 30°C and 180 rpm using YPD medium (1% yeast extract, 2% peptone and 2% glucose). For Opi⁻ plate tests we additionally used non-buffered, threonine-free minimal SD media composed of 0.67% yeast nitrogen base with ammonium sulfate, 2% glucose, vitamins, trace elements and amino acids, with 75 µM inositol (+Ino) or without inositol (-Ino) as described in (Villa-García *et al.*, 2011). Solid media contained 2% agar.

Soraphen A (SorA), an Acc1-specific oligomerisation inhibitor was kindly provided by Dr. Gerth, Helmholtz-Zentrum für Infektionsforschung, Germany

To calculate the doubling times cells were pre-cultivated for 72 h in liquid YPD medium to stationary growth phase and then rediluted to OD_{600} = 0.25 in 50 mL of fresh YPD medium. OD_{600} was measured after 3.0, 4.5, 6.0, 7.5, 9.0, 12 and 15 hours of growth. Doubling times were determined as described in (Gaspar *et al.*, 2011).

For lipid extraction, protein- and oligomer analysis as well as for microscopy and immuno staining cells were grown for 16 h in YPD medium to mid-logarithmic growth phase, rediluted to OD_{600} = 0.5 in fresh YPD medium and grown for 5 h to the early logarithmic growth phase with an OD_{600} ≈ 4. Pellets of 20 OD_{600} units were harvested (3,500 rpm, 5 min) and stored at -80°C for later protein and lipid analysis.

4.3 Phenotypic characterization

For plate tests, cells were grown for 16 hours in YPD medium, harvested and washed twice with water. 5 µl of serial 1:10 dilutions starting with OD_{600} = 1/mL were spotted on the indicated media. Plates were analysed after 2 days of growth at 30°C.

4.4 Microscopy

Microscopy was performed using a Leica SP2 confocal microscope (Leica Microsystems, Mannheim, Germany) with spectral detection and a Leica 100x immersion objective (NA=1.4). Cells were subjected to microscopy at the indicated time points grown in fresh YPD after pre-cultivation for 16 hours. Fluorescence of the GFP fusion proteins was excited at 488 nm, GFP fluorescence emission was detected in the range between 500-550 nm. Fluorescence of the RFP fusion proteins was excited at 561 nm, RFP fluorescence emission was detected in the range between 575-650 nm. Transmission images were recorded using differential interference contrast (DIC) optics.

4.5 Immuno staining

4.5.1 Fixation

Cells were grown as described in 4.2 to an OD_{600} ≈ 5. 1mL of the cell suspension was treated with 1 mL of EGTA [150 mM, pH 7 (KOH)] and 10µL Pepstatin [1mg/mL in MeOH]. After 5 min of incubation 5 mL of 7.4% (w/v) formaldehyde in 2xPEM

Buffer [0.2 M PIPES, 10 mM EGTA, 10mM $MgCl_2$, pH 6.9 (KOH)] was added, the cells were fixed for 45 min. on a reciprocal shaker and washed 3 times with 4xPEM buffer (1000 x g, 4 min)

4.5.2 Permeabilisation

Fixed cells were washed with KCP buffer [0.1M KH_2PO_4, 0.1 M citric acid pH 5.9 (KOH)] and resuspended in 1 mL KCP buffer with 5µL 2-mercaptoethanol and 50µL zymolyase [1 mg/mL zymolyase-20T in KCP]. The mixture was incubated at 30°C for 30 min, subsequently centrifuged (1,000 x g, 4 min) and washed twice with 4xPEM. The cells were permeabilised with 20 µL Triton X-100 solution [0.5% (v/v) in 4xPEM] and washed with 1mL 4xPEM (1,000 x g, 4 min).

4.5.3 Incubation with antibodys

The pellet was resuspendet in 500 µL BSA [2% (v/v) in 4xPEM], incubated for 20 min at room temperature (RT), and treaded with mouse anti Acc1 primary antibody [1:500 in 4xPEM] for 60 min at room temperature. The cells were washed 3 times with 4xPEM (1000 x g, 4 min.), and incubated for 60 min with anti mouse Alexa-Fluor secondary antibody [1:200 (v/v) in 1% BSA/4xPEM] at RT. After incubation the antibody was removed by centrifugation (1,000 x g, 4 min), the cells were washed 3 times with 4xPEM (1,000 x g, 4 min) and afterwards subjected to confocal laser scanning microscopy using a Leica SP5 confocal microscope (Leica Microsystems, Mannheim, Germany)

4.6 Determination of lipid profiles and fatty acid composition

4.6.1 Lipid extraction

Cells were grown as described in 4.2 and 20 OD_{600} units were harvested after 5 h of growth. The harvested cells were resuspended in 5 mL chloroform/methanol 2:1 (v/v) and disintegrated with glass beads on a Multi Reax vibrating shaker (Heidolph Inc., Schwabach, Germany). Lipids were extracted according to a slightly modified Folch method (Folch *et al.*, 1957; Schneiter and Daum, 2006) with addition of an internal standard mix containing TAG 45:0, TAG 51:0, TAG 57:0, DAG 36:0, DAG28:0, PC 24:0, PC 34:0, PC 38:0, PE 24:0, PE 34:0 (Knittelfelder *et al.*, 2014).

4.6.2 Thin layer chromatography (TLC)

Thin layer chromatography was performed by applying 25 µL of lipid extract on a silica gel TLC plate (Merck, TLC silica gel 60 F_{254}) with a CAMAG TLC sampler 4. As

reference 15 µL of a standard mix containing TAG, SE and Erg were applied to the TLC plate. The samples were separated using a mixture of petrolether/diethylether/acetic acid (32/8/0.4) and visualized using a H_2SO_4 containing dipping solution ($MnCl_2$/H_2O/EtOH/H_2SO_4) (5.04 g/480 mL/480 mL/32 mL).

4.6.3 Phospholipid and neutral lipid analysis using an UPLC-Synapt qTOF HDMS system

Phospholipid and neutral lipid analyses were performed on a UPLC-Synapt qTOF HDMS system (Waters, Manchester, United Kingdom) as described by Knittelfelder et al. (Knittelfelder *et al.*, 2014).

4.6.4 Phospholipid and neutral lipid analysis using an Agilent 1100 HPLC system with evaporative light scattering detector (ELSD)

Quantitative HPLC analysis of TAG, SE and PC was performed on an Agilent 1100 HPLC system with a Sedex 85 ELSD (Sedere, France). Standard curves were derived from dilutions of cholesterol palmitate, TAG (48:3) and PC (34:1) standards, ranging from 5.5 µg/ml to 350 µg/ml.

210 µL lipid extract were dried under a stream of nitrogen and dissolved in 70 µL chloroform/methanol (2/1). 10 µL of the solution were injected and separated on a BETASIL Diol-100 column (150x4.6, 5 µm particel size, Thermo scientific) at 40°C. The separation was carried out for 49 min using a ternary gradient consisting of eluent A: isooctane/ethyl acetate (99.8/0.2), eluent B: acetone/ ethyl acetate/ acetic acid) (2/1/0.02%) and eluent C: isopropanol/water/acetic acid/ammonium acetate (85/15/0.05%/0.3%)

4.6.5 Fatty acid analysis was performed on a Thermo Trace GC Ultra GC-MS system after generation of fatty acid methyl esters using HCl/MeOH.

A 200 µl aliquot of the lipid extract containing the internal standard mix was used for methyl ester production and GC-MS measurements of total fatty acid and FA composition. To prevent lipid oxidation, 100 µg of butylhydroxytoluene (BHT) were added to the samples which were then dried under a stream of nitrogen and re-dissolved in 0.5 ml toluene. Thereafter 3 ml of 2% HCl in methanol were added and incubated for 1 hour at 100°C. After incubation the samples were immediately cooled on ice, 1 ml of ice-cold water and 2 ml of hexane/chloroform 4:1 (v/v) were added and mixed on an overhead shaker for 15 min. To separate the phases the samples were centrifuged at 3,000 rpm for 3 min and the organic upper phase was collected. The

aqueous phase was washed using 1 ml ice-cold water and 2 ml of hexane/chloroform 4:1 (v/v) and centrifugation at 3,000 rpm for 3 min. Again the organic upper phase was collected, pooled with the first organic phase and dried under a stream of nitrogen. Methyl esters were dissolved in 100 µl hexane and analyzed using gas chromatography – mass spectrometry (GC-MS). A sample volume of 1 µl was injected at an injector temperature of 250°C. Samples were separated with a temperature gradient from 110 to 300°C using a HP-5MS column with 60 m length and 0.25 mm inner diameter (Agilent, Waldbronn, Germany) and helium as carrier gas on a TRACE GC Ultra gas chromatograph (Thermo Scientific, Waltham, USA). Sample analysis was performed on a DSQ mass spectrometer using the Xcalibur software (Thermo Scientific). Calibration curves were obtained by using standards of free fatty acids (FFA) for all analysed FA species. The FFA were converted into methyl esters according to the same protocol.

4.7 Determination of protein levels and oligomerisation by Western blot analysis

4.7.1 Protein preparation

Cells were grown as described in 4.2. The harvested pellet was resuspended in 800 µL Tris/Cl (10 mM, pH7.4) and transferred to a 1.5 mL screwcap-Eppendorf tube with 150 µL glass beads. To prevent degradation of proteins 0.8 µL of a protease inhibitor mixture were added. The cells were disintegrated for 3 min (cooling every 30 s with CO_2) using a Merckenschlager disintegrator. The cell lysate was subjected to different centrifugation steps to yield different cellular compartments. The first fraction (pellet) was obtained by centrifugation at 1,200g, the second fraction yielded the membrane pellet at 16,000g and the supernatant containing the non sedimentable proteins was referred to as cytosolic fraction.

4.7.2 SDS Gel

The fractions from 4.7.1 were dissolved in Tris/Cl (10 mM, pH7.4) and TCA (50%) to a final concentration of 12.5% TCA. The suspension was then stored at -20°C for at least 16 h. The precipitate was spun down at 16,000g at 4°C, and washed twice with 500 µL ice cold acetone (80%) (16,000g, 4°C). The supernatant was carefully removed with a pipette tip and the pellet was air dried for not longer than 5 min. Afterwards the pellet was dissolved in 100 µL 1% SDS/0.1N NaOH and 100 µL 2x sample buffer (0.125 M Tris/Cl pH 6.8, 4 % SDS, 20 % Glycerol, 0.02 % bromphenol

blue, 5 % β mercapto ethanol), boiled at 95°C for 5 min and loaded onto a 10% SDS-PA gel (0,57 M Tris/Cl pH 8.8, 0.1% SDS, 0.1% TEMED, 0.05 % APS) with 5% collection gel (0.06 M Tris/Cl pH 6.8, 0.1% SDS, 0.1% TEMED, 0.05% APS). The gels were run at 30 mA/gel, using a tris-glycin running buffer (25 mM Tris, 192 mM glycine, 0.1% SDS)

4.7.3 Native gradient gels

To separate native oligomeric Acc1 complexes a 4-8% gradient acrylamide gel without SDS was prepared by mixing 8% acrylamide solution (0.56 M Tris/Cl pH 6.8,0.05% TEMED, 0.03% APS) with 4% acrylamide solution (0.56 M Tris/Cl pH 6.8, 0.05% TEMED, 0.04% APS) using a gradient mixer. The collecting gel consisted of a 3.2% acrylamide gel (0.06 M Tris/Cl pH 8.8, 0.1% TEMED, 0.05% APS)

The cytosolic fraction from 4.7.1 was mixed with 10x native loading buffer (70% glycerol, 0.2% coomassie-blue G250 dissolved in 10 mM Tris/Cl, pH 7.4), the pellet fraction was suspended in 800 µL Tris/Cl (10 mM, pH 7.4) and 0.8 µL protease inhibitor mixture and mixed with 10x native loading buffer.

The mitochondrial fraction was treated with 40 µL Triton® X-100 (6% in 10 mM Tris/Cl, pH7.4) to yield a final concentration of 1g Triton® X-100 per 1g membrane pellet and incubated for 15 min at RT. Thereafter the mixture was treated with 10x native loading buffer.

All prepared fractions were applied on the native gradient gel and run at 100 V for approximately 30 min until the protein front reached the separation gel; thereafter the voltage was increased to 180 V for another 2.5 hours. The electrophoresis process was carried out at 4°C, using a tris-glycin running buffer without SDS (25 mM Tris, 192 mM glycine).

4.7.4 Protein transfer and Western blot analysis

Polyacrylamide gels from 4.7.2 and 4.7.3 were subjected to Western blot analysis in a sandwich assembled electrophoresis transfer to a nitrocellulose membrane (0.45 µm, Biorad) The transfer of the Proteins was performed at 150 mA for 2 hours (4°C) in transfer buffer (25 mM Tris, 192 mM glycine, 20% methanol, 0.01% SDS). Afterwards membranes were stained with PonceauS, washed with water and blocked in 5% milk powder in TTBS (50mM Tris, 150 mM NaCl, 0.1% tween 20, pH 8) for 1 hour. The primary mouse anti Acc1 antibody was applied (1:1,000 in 2.5% milk

powder in TTBS) for 1 hour at 4°C. After washing the membrane (3 times, 10 min each, with TTBS) the anti mouse secondary POD antibody was applied (1:7,500 in 2.5% milk powder in TTBS) for 1 hour at 4°C. As a loading control the membranes were treated with a primary rabbit GapDH antibody (1:60,000 in 2.5% milk powder in TTBS) and the corresponding anti rabbit POD secondary antibody (1:7,500 in 2.5% milk powder in TTBS). The membranes were again washed as before, overlayered with 2 mL "Thermo supersignal west pico chemiluminescent substrate" luminol/enhancer mix (1:1) and detected on a film.

4.7.5 Soraphen A treatment of cells in liquid media

Cells were pre-cultured for 16 hours as described in 4.2, rediluted in fresh YPD and grown for 1.5 hours. SorA was added as indicated to the medium, cells were grown for another 1.5 hours, harvested and subjected to SDS-PAGE and Western blotting as described in 4.7.

4.8 Chemicals

Table 2. Chemicals used in this study

Acetic acid (glacial)	Merck
Acetone	Roth
Acrylamid 40%	Bio-Rad
Adenine	Sigma Aldrich
Ammonium acetate	Fluka
Ammonium persulphate	Bio-Rad
Ammonium sulphate	Roth
Anti-Acc1 antibody	
Anti-GAPDH antibody	home source
Anti-mouse POD antibody	Pierce
Anti-mouse antibody Alexa Fluor 568	Molecular Probes
Anti-rabbit POD antibody	Pierce
Arginine	Merck
Biotin	Merck
Calcium chloride	Fluka
Calicum pantothenate	Acros Organics
Chloroform	Sigma Aldrich
Cholesterylpalmitate	Sigma Aldrich
Citric acid	Roth
Copper sulphate	Merck
EGTA	Sigma Aldrich
Ethylacetate	Merck
Folic acid	Sigma Aldrich
Formic acid	Merck
Glass beads	Sartorius
Glucose mono hydrate	Roth
Glycine	AppliChem

Histidine monohydrochloride	Merck
Inositol	Sigma Aldrich
Iron chloride	Merck
Isopropanol	Roth
Leucine	Sigma Aldrich
Leucine enkephalin	Sigma Aldrich
Lysine monohydrochloride	Merck
Magnesium chloride	Merck
Magnesium sulphate	Roth
Manganese sulphate	J.T. Baker
2-mercapto ethanol	Merck
Methanol	J.T. Baker
Methionine	Merck
Milk powder	Roth
NaCl	Roth
NaOH	Merck
n-Hexane	Roth
Niacin	Fluka
Optical adhesive covers	Applied Biosystems
p-Aminobenzoic acid	Sigma Aldrich
Paraformaldehyde	Merck
Peptone	BD
PIPES	Merck
Potassium dihydrogen phosphate	Roth
Potassium hydroxide	Merck
Potassium iodide	Merck
Pyridoxal hydrochloride	Calbiochem
Riboflavin	Sigma Aldrich
SDS	Sigma Aldrich
Sodium molybdate	Merck
Super signalWest Pico chemiluminscent Substrate	Thermo Scientific
TEMED	Roth
Thiamine hydrochloride	Sigma Aldrich
Toluene	Merck
Trichloroacetic acid	Merck
Tris	Roth
Triton X-100	Sigma
Tryptophan	Merck
Tween 20	Merck
Uracil	Sigma Aldrich
Water	in-house distillery
Yeast extract	BD
Zinc sulfate	Roth
Zymolyase	Sikagaku Biosystems

5 Literature

Al-Feel, W., DeMar, J. C., and Wakil, S. J. (2003). A Saccharomyces cerevisiae mutant strain defective in acetyl-CoA carboxylase arrests at the G2/M phase of the cell cycle. Proc. Natl. Acad. Sci. U. S. A. *100*, 3095–3100.

Bandyopadhyay, S. *et al.* (2006). Mechanism of apoptosis induced by the inhibition of fatty acid synthase in breast cancer cells. Cancer Res. *66*, 5934–5940.

Beckers, A., Organe, S., Timmermans, L., Scheys, K., Peeters, A., Brusselmans, K., Verhoeven, G., and Swinnen, J. V (2007). Chemical inhibition of acetyl-CoA carboxylase induces growth arrest and cytotoxicity selectively in cancer cells. Cancer Res. *67*, 8180–8187.

Bertin, A., McMurray, M. A., Pierson, J., Thai, L., McDonald, K. L., Zehr, E. A., García, G., Peters, P., Thorner, J., and Nogales, E. (2012). Three-dimensional ultrastructure of the septin filament network in Saccharomyces cerevisiae. Mol. Biol. Cell *23*, 423–432.

Black, P. N., and DiRusso, C. C. (2007). Yeast acyl-CoA synthetases at the crossroads of fatty acid metabolism and regulation. Biochim. Biophys. Acta *1771*, 286–298.

Borthwick, A. C., Edgell, N. J., and Denton, R. M. (1987). Use of rapid gel-permeation chromatography to explore the inter-relationships between polymerization, phosphorylation and activity of acetyl-CoA carboxylase. Effects of insulin and phosphorylation by cyclic AMP-dependent protein kinase. Biochem. J. *241*, 773–782.

Botstein, D., and Fink, G. R. (2011). Yeast: an experimental organism for 21st Century biology. Genetics *189*, 695–704.

Boumann, H. A., Gubbens, J., Koorengevel, M. C., Oh, C.-S., Martin, C. E., Heck, A. J. R., Patton-Vogt, J., Henry, S. A., de Kruijff, B., and de Kroon, A. I. P. M. (2006). Depletion of phosphatidylcholine in yeast induces shortening and increased saturation of the lipid acyl chains: evidence for regulation of intrinsic membrane curvature in a eukaryote. Mol. Biol. Cell *17*, 1006–1017.

Bozaquel-Morais, B. L., Madeira, J. B., Maya-Monteiro, C. M., Masuda, C. A., and Montero-Lomeli, M. (2010). A new fluorescence-based method identifies protein phosphatases regulating lipid droplet metabolism. PLoS One *5*, e13692.

Brinkworth, R. I., Munn, A. L., and Kobe, B. (2006). Protein kinases associated with the yeast phosphoproteome. BMC Bioinformatics *7*, 47.

Brusselmans, K., De Schrijver, E., Verhoeven, G., and Swinnen, J. V (2005). RNA interference-mediated silencing of the acetyl-CoA-carboxylase-alpha gene induces growth inhibition and apoptosis of prostate cancer cells. Cancer Res. *65*, 6719–6725.

Cáp, M., Stěpánek, L., Harant, K., Váchová, L., and Palková, Z. (2012). Cell differentiation within a yeast colony: metabolic and regulatory parallels with a tumor-affected organism. Mol. Cell *46*, 436–448.

Carman, G. M., and Han, G.-S. (2009). Regulation of phospholipid synthesis in yeast. J. Lipid Res. *50 Suppl*, S69–73.

Carmona-Gutierrez, D., Eisenberg, T., Büttner, S., Meisinger, C., Kroemer, G., and Madeo, F. (2010). Apoptosis in yeast: triggers, pathways, subroutines. Cell Death Differ. *17*, 763–773.

Chajès, V., Cambot, M., Moreau, K., Lenoir, G. M., and Joulin, V. (2006). Acetyl-CoA carboxylase alpha is essential to breast cancer cell survival. Cancer Res. *66*, 5287–5294.

Cheng, J.-F. *et al.* (2006). Synthesis and structure-activity relationship of small-molecule malonyl coenzyme A decarboxylase inhibitors. J. Med. Chem. *49*, 1517–1525.

Chirala, S. S., Zhong, Q., Huang, W., and al-Feel, W. (1994). Analysis of FAS3/ACC regulatory region of Saccharomyces cerevisiae: identification of a functional UASINO and sequences responsible for fatty acid mediated repression. Nucleic Acids Res. *22*, 412–418.

Chou, C.-Y., Yu, L. P. C., and Tong, L. (2009). Crystal structure of biotin carboxylase in complex with substrates and implications for its catalytic mechanism. J. Biol. Chem. *284*, 11690–11697.

Colbert, C. L., Kim, C.-W., Moon, Y.-A., Henry, L., Palnitkar, M., McKean, W. B., Fitzgerald, K., Deisenhofer, J., Horton, J. D., and Kwon, H. J. (2010). Crystal structure of Spot 14, a modulator of fatty acid synthesis. Proc. Natl. Acad. Sci. U. S. A. *107*, 18820–18825.

Davies, S. P., Sim, A. T., and Hardie, D. G. (1990). Location and function of three sites phosphorylated on rat acetyl-CoA carboxylase by the AMP-activated protein kinase. Eur. J. Biochem. *187*, 183–190.

Ejsing, C. S., Sampaio, J. L., Surendranath, V., Duchoslav, E., Ekroos, K., Klemm, R. W., Simons, K., and Shevchenko, A. (2009). Global analysis of the yeast lipidome by quantitative shotgun mass spectrometry. Proc. Natl. Acad. Sci. U. S. A. *106*, 2136–2141.

Fiala, G. J., Schamel, W. W. A., and Blumenthal, B. (2011). Blue native polyacrylamide gel electrophoresis (BN-PAGE) for analysis of multiprotein complexes from cellular lysates. J. Vis. Exp., e2164.

Ficarro, S. B., McCleland, M. L., Stukenberg, P. T., Burke, D. J., Ross, M. M., Shabanowitz, J., Hunt, D. F., and White, F. M. (2002). Phosphoproteome analysis by mass spectrometry and its application to Saccharomyces cerevisiae. Nat. Biotechnol. *20*, 301–305.

Folch, J., LEES, M., and SLOANE STANLEY, G. H. (1957). A simple method for the isolation and purification of total lipides from animal tissues. J. Biol. Chem. *226*, 497–509.

Galdieri, L., and Vancura, A. (2012). Acetyl-CoA carboxylase regulates global histone acetylation. J. Biol. Chem. *287*, 23865–23876.

Garcia, G., Bertin, A., Li, Z., Song, Y., McMurray, M. A., Thorner, J., and Nogales, E. (2011). Subunit-dependent modulation of septin assembly: budding yeast septin Shs1 promotes ring and gauze formation. J. Cell Biol. *195*, 993–1004.

Gaspar, M. L., Hofbauer, H. F., Kohlwein, S. D., and Henry, S. A. (2011). Coordination of storage lipid synthesis and membrane biogenesis: evidence for cross-talk between triacylglycerol metabolism and phosphatidylinositol synthesis. J. Biol. Chem. *286*, 1696–1708.

Gladfelter, A. S., Pringle, J. R., and Lew, D. J. (2001). The septin cortex at the yeast mother-bud neck. Curr. Opin. Microbiol. *4*, 681–689.

Ha, J., Daniel, S., Broyles, S., and Kim, K. (1994). Critical phosphorylation sites for acetyl-CoA carboxylase activity. J. Biol. Chem. *269*, 22162–22168.

Hanahan, D., and Weinberg, R. A. (2000). The hallmarks of cancer. Cell *100*, 57–70.

Hanahan, D., and Weinberg, R. A. (2011). Hallmarks of cancer: the next generation. Cell *144*, 646–674.

Hasslacher, M., Ivessa, A. S., Paltauf, F., and Kohlwein, S. D. (1993). Acetyl-CoA carboxylase from yeast is an essential enzyme and is regulated by factors that control phospholipid metabolism. J. Biol. Chem. *268*, 10946–10952.

Henry, S. A., Kohlwein, S. D., and Carman, G. M. (2012). Metabolism and regulation of glycerolipids in the yeast Saccharomyces cerevisiae. Genetics *190*, 317–349.

Hildreth, K. L., Van Pelt, R. E., and Schwartz, R. S. (2012). Obesity, insulin resistance, and Alzheimer's disease. Obesity (Silver Spring). *20*, 1549–1557.

Hofbauer, H. F. (2012). Keeping the balance! A crucial role of lipid fatty acid composition to maintain cell viability. University of Graz.

Johansson, P., Wiltschi, B., Kumari, P., Kessler, B., Vonrhein, C., Vonck, J., Oesterhelt, D., and Grininger, M. (2008). Inhibition of the fungal fatty acid synthase type I multienzyme complex. Proc. Natl. Acad. Sci. U. S. A. *105*, 12803–12808.

Jump, D. B., Torres-Gonzalez, M., and Olson, L. K. (2011). Soraphen A, an inhibitor of acetyl CoA carboxylase activity, interferes with fatty acid elongation. Biochem. Pharmacol. *81*, 649–660.

Kim, C.-W., Moon, Y.-A., Park, S. W., Cheng, D., Kwon, H. J., and Horton, J. D. (2010). Induced polymerization of mammalian acetyl-CoA carboxylase by MIG12

provides a tertiary level of regulation of fatty acid synthesis. Proc. Natl. Acad. Sci. U. S. A. *107*, 9626–9631.

Knittelfelder, O. L., Weberhofer, B. P., Eichmann, T. O., Kohlwein, S. D., and Rechberger, G. N. (2014). A versatile ultra-high performance LC-MS method for lipid profiling. J. Chromatogr. B *951-952*, 119–128.

Kridel, S. J., Axelrod, F., Rozenkrantz, N., and Smith, J. W. (2004). Orlistat Is a Novel Inhibitor of Fatty Acid Synthase with Antitumor Activity Orlistat Is a Novel Inhibitor of Fatty Acid Synthase with Antitumor Activity. 2070–2075.

De Kroon, A. I. P. M., Rijken, P. J., and De Smet, C. H. (2013). Checks and balances in membrane phospholipid class and acyl chain homeostasis, the yeast perspective. Prog. Lipid Res. *52*, 374–394.

Kuhajda, F. P. (2000). Fatty-acid synthase and human cancer: new perspectives on its role in tumor biology. Nutrition *16*, 202–208.

Lampl, M. (1998). Function of acetyl-CoA carboxylase in the yeast Saccharomyces cerevisiae. Graz University of Technology.

Lee, E. B. (2011). Obesity, leptin, and Alzheimer's disease. Ann. N. Y. Acad. Sci. *1243*, 15–29.

Letra, L., Santana, I., and Seiça, R. (2014). Obesity as a risk factor for Alzheimer's disease: the role of adipocytokines. Metab. Brain Dis.

Locke, G. A., Cheng, D., Witmer, M. R., Tamura, J. K., Haque, T., Carney, R. F., Rendina, A. R., and Marcinkeviciene, J. (2008). Differential activation of recombinant human acetyl-CoA carboxylases 1 and 2 by citrate. Arch. Biochem. Biophys. *475*, 72–79.

Longtine, M. S., DeMarini, D. J., Valencik, M. L., Al-Awar, O. S., Fares, H., De Virgilio, C., and Pringle, J. R. (1996). The septins: roles in cytokinesis and other processes. Curr. Opin. Cell Biol. *8*, 106–119.

Martel, P., Bingham, C., Mcgraw, C., Baker, C., Morganelli, P., Meng, M., Armstrong, J., Moncur, J., and Kinlaw, W. (2005). S14 protein in breast cancer cells: Direct evidence of regulation by SREBP-1c, superinduction with progestin, and effects on cell growth. Exp. Cell Res. *312*, 278–288.

Martin, C. E., Oh, C.-S., and Jiang, Y. (2007). Regulation of long chain unsaturated fatty acid synthesis in yeast. Biochim. Biophys. Acta *1771*, 271–285.

Mishina, M., Roggenkamp, R., and Schweizer, E. (1980). Yeast mutants defective in acetyl-coenzyme A carboxylase and biotin: apocarboxylase ligase. Eur. J. Biochem. *111*, 79–87.

Munday, M. R. (2002). Regulation of mammalian acetyl-CoA carboxylase. Biochem. Soc. Trans. *30*, 1059–1064.

Natter, K., and Kohlwein, S. D. (2013). Yeast and cancer cells - common principles in lipid metabolism. Biochim. Biophys. Acta *1831*, 314–326.

Numa, S., Bortz, W. M., and Lynen, F. (1965). Regulation of fatty acid synthesis at the acetyl-CoA carboxylation step. Adv. Enzyme Regul. *3*, 407–423.

Park, S., Hwang, I.-W., Makishima, Y., Perales-Clemente, E., Kato, T., Niederländer, N. J., Park, E. Y., and Terzic, A. (2013). Spot14/Mig12 heterocomplex sequesters polymerization and restrains catalytic function of human acetyl-CoA carboxylase 2. J. Mol. Recognit. *26*, 679–688.

Patton-Vogt, J., Griac, P., and Sreenivas, A. (1997). Role of the Yeast Phosphatidylinositol/Phosphatidylcholine Transfer Protein (Sec14p) in Phosphatidylcholine Turnover andINO1 Regulation. J. Biol. ….

Pizer, E. S., Jackisch, C., Wood, F. D., Pasternack, G. R., Davidson, N. E., and Kuhajda, F. P. (1996a). Inhibition of fatty acid synthesis induces programmed cell death in human breast cancer cells. Cancer Res. *56*, 2745–2747.

Pizer, E. S., Wood, F. D., Heine, H. S., Romantsev, F. E., Pasternack, G. R., and Kuhajda, F. P. (1996b). Inhibition of fatty acid synthesis delays disease progression in a xenograft model of ovarian cancer. Cancer Res. *56*, 1189–1193.

Remington, S. J. (2011). Green fluorescent protein: a perspective. Protein Sci. *20*, 1509–1519.

Sampaio, J. L., Gerl, M. J., Klose, C., Ejsing, C. S., Beug, H., Simons, K., and Shevchenko, A. (2011). Membrane lipidome of an epithelial cell line. Proc. Natl. Acad. Sci. U. S. A. *108*, 1903–1907.

Schneiter, R., and Daum, G. (2006). Analysis of yeast lipids. Methods Mol. Biol. *313*, 75–84.

Schneiter, R., Hitomi, M., Ivessa, A. S., Fasch, E. V, Kohlwein, S. D., and Tartakoff, A. M. (1996). A yeast acetyl coenzyme A carboxylase mutant links very-long-chain fatty acid synthesis to the structure and function of the nuclear membrane-pore complex. Mol. Cell. Biol. *16*, 7161–7172.

Shaner, N. C., Steinbach, P. A., and Tsien, R. Y. (2005). A guide to choosing fluorescent proteins. Nat. Methods *2*, 905–909.

Shen, Y., Volrath, S. L., Weatherly, S. C., Elich, T. D., and Tong, L. (2004). A mechanism for the potent inhibition of eukaryotic acetyl-coenzyme A carboxylase by soraphen A, a macrocyclic polyketide natural product. Mol. Cell *16*, 881–891.

Sherman, F. (2002). Getting started with yeast. Methods Enzymol. *350*, 3–41.

Shirra, M. K., Patton-Vogt, J., Ulrich, A., Liuta-Tehlivets, O., Kohlwein, S. D., Henry, S. A., and Arndt, K. M. (2001). Inhibition of acetyl coenzyme A carboxylase activity restores expression of the INO1 gene in a snf1 mutant strain of Saccharomyces cerevisiae. Mol. Cell. Biol. *21*, 5710–5722.

De Smet, C. H., Vittone, E., Scherer, M., Houweling, M., Liebisch, G., Brouwers, J. F., and de Kroon, A. I. P. M. (2012). The yeast acyltransferase Sct1p regulates fatty acid desaturation by competing with the desaturase Ole1p. Mol. Biol. Cell *23*, 1146–1156.

Tanaka-Takiguchi, Y., Kinoshita, M., and Takiguchi, K. (2009). Septin-mediated uniform bracing of phospholipid membranes. Curr. Biol. *19*, 140–145.

Tatzer, V., Zellnig, G., Kohlwein, S. D., and Schneiter, R. (2002). Lipid-dependent subcellular relocalization of the acyl chain desaturase in yeast. Mol. Biol. Cell *13*, 4429–4442.

Tehlivets, O., Scheuringer, K., and Kohlwein, S. D. (2007). Fatty acid synthesis and elongation in yeast. Biochim. Biophys. Acta *1771*, 255–270.

Thampy, K. G., and Wakil, S. J. (1985). Activation of Acetyl-coA Carboxylase. J. Biol. Chem. *260*, 6318–6323.

Toh, H., Kondo, H., and Tanabe, T. (1993). Molecular evolution of biotin-dependent carboxylases. Eur. J. Biochem. *215*, 687–696.

Tong, L. (2005). Acetyl-coenzyme A carboxylase: crucial metabolic enzyme and attractive target for drug discovery. Cell. Mol. Life Sci. *62*, 1784–1803.

Tong, L., and Harwood, H. J. (2006). Acetyl-coenzyme A carboxylases: versatile targets for drug discovery. J. Cell. Biochem. *99*, 1476–1488.

Vahlensieck, H. F., Pridzun, L., Reichenbach, H., and Hinnen, A. (1994). Identification of the yeast ACC1 gene product (acetyl-CoA carboxylase) as the target of the polyketide fungicide soraphen A. Curr. Genet. *25*, 95–100.

Vazquez-Martin, A., Corominas-Faja, B., Oliveras-Ferraros, C., Cufí, S., Dalla Venezia, N., and Menendez, J. A. (2013). Serine79-phosphorylated acetyl-CoA carboxylase, a downstream target of AMPK, localizes to the mitotic spindle poles and the cytokinesis furrow. Cell Cycle *12*, 1639–1641.

Villa-García, M. J., Choi, M. S., Hinz, F. I., Gaspar, M. L., Jesch, S. A., and Henry, S. A. (2011). Genome-wide screen for inositol auxotrophy in Saccharomyces cerevisiae implicates lipid metabolism in stress response signaling. Mol. Genet. Genomics *285*, 125–149.

Wang, C., Xu, C., Sun, M., Luo, D., Liao, D., and Cao, D. (2009). Acetyl-CoA carboxylase-alpha inhibitor TOFA induces human cancer cell apoptosis. Biochem. Biophys. Res. Commun. *385*, 302–306.

Warenda, A. J., and Konopka, J. B. (2002). Septin function in Candida albicans morphogenesis. Mol. Biol. Cell *13*, 2732–2746.

Weatherly, S. C., Volrath, S. L., and Elich, T. D. (2004). Expression and characterization of recombinant fungal acetyl-CoA carboxylase and isolation of a soraphen-binding domain. Biochem. J. *380*, 105–110.

WHO http://www.euro.who.int/en/health-topics/noncommunicable-diseases/obesity. [Accessed 18.02.2014]

WHO http://www.euro.who.int/en/health-topics/noncommunicable-diseases/obesity/data-and-statistics. [Accessed 11.03.2014]

WHO http://www.who.int/cancer/prevention/en/. [Accessed 18.02.2014]

WHO http://www.who.int/mediacentre/factsheets/fs297/en/. [Accessed 21.02.2014]

WHO http://www.who.int/mediacentre/factsheets/fs310/en/.[Accessed 22.01.2014]

WHO http://www.who.int/mediacentre/factsheets/fs311/en/index.html. [Accessed 18.02.2014]

WHO http://www.wpro.who.int/mediacentre/factsheets/obesity/en/index.html. [Accessed 22.01.2014]

Winzeler, E. A. *et al.* (1999). Functional characterization of the S. cerevisiae genome by gene deletion and parallel analysis. Science *285*, 901–906.

Woods, A., Munday, M. R., Scott, J., Yang, X., Carlson, M., and Carling, D. (1994). Yeast SNF1 is functionally related to mammalian AMP-activated protein kinase and regulates acetyl-CoA carboxylase in vivo. J. Biol. Chem. *269*, 19509–19515.

Zhang, H., Yang, Z., Shen, Y., and Tong, L. (2003). Crystal structure of the carboxyltransferase domain of acetyl-coenzyme A carboxylase. Science *299*, 2064–2067.

Zhang, M., Galdieri, L., and Vancura, A. (2013). The yeast AMPK homolog SNF1 regulates acetyl coenzyme A homeostasis and histone acetylation. Mol. Cell. Biol. *33*, 4701–4717.

Zou, Z., Tong, F., Faergeman, N. J., Børsting, C., Black, P. N., and DiRusso, C. C. (2003). Vectorial acylation in Saccharomyces cerevisiae. Fat1p and fatty acyl-CoA synthetase are interacting components of a fatty acid import complex. J. Biol. Chem. *278*, 16414–16422.